

114 天氣分析與預報研討會 — *Sep 4th 2025*

應用自組織映射圖分類法客觀辨識東亞地區之春夏季節演變

Identifying the East Asia Spring-to-Summer Transition Using Self-Organizing Map

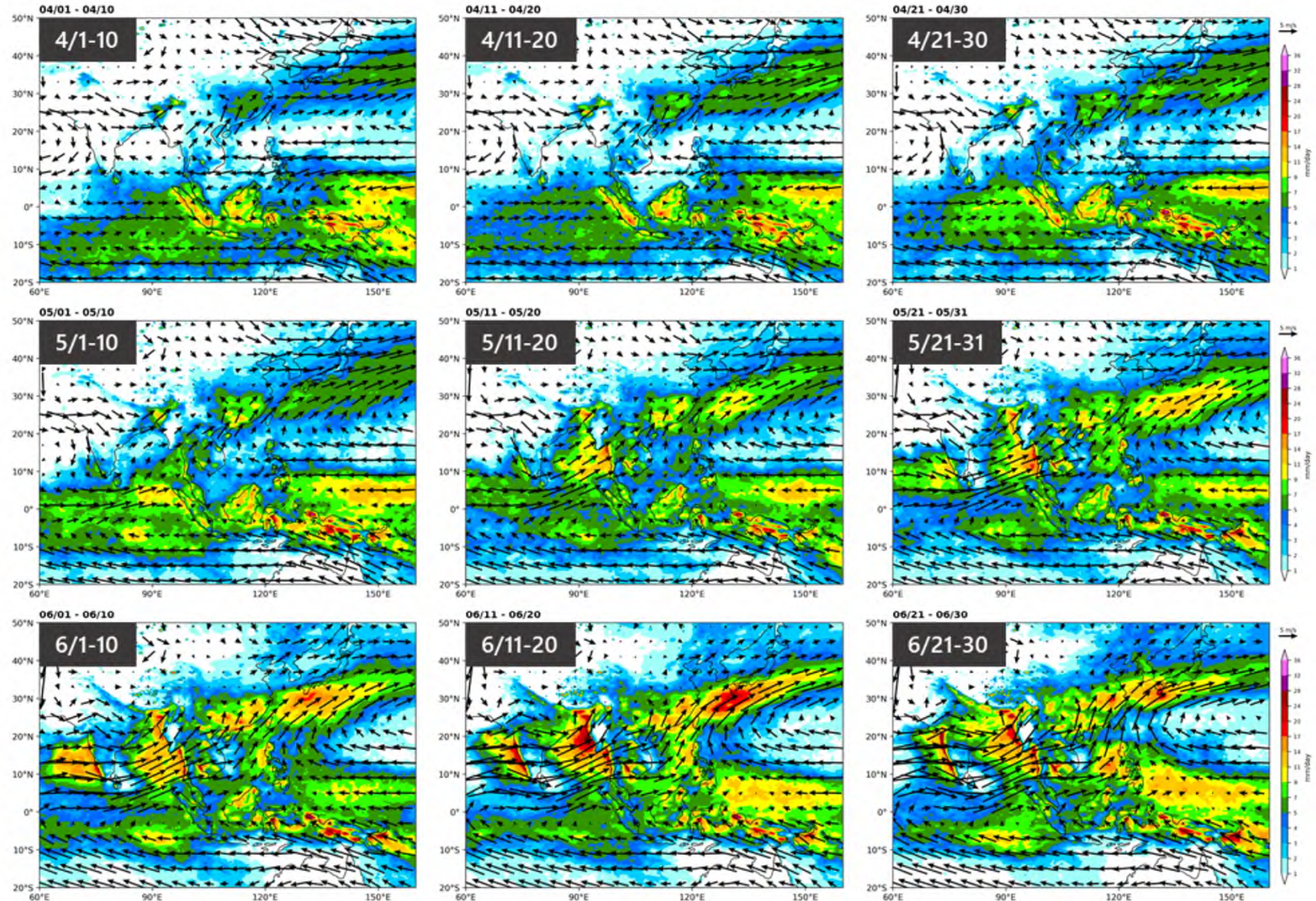
黃聖丰¹ 盧孟明² 羅資婷¹

¹中央氣象署海象氣候組 ²國立臺灣大學

Outline

- Introduction
- Research Objectives
- Data and Methodology
- Results
 - 01 - Three Development Stages of EAM
 - 02 - ENSO Modulations on EAM
 - 03 - SOM WTs and Taiwan-Philippine Extreme Weather
- Conclusions & Future Works
- References

- Substantial change of low-level wind and precipitation exhibits during spring-to-summer transition. [Ding and Chan 2005]

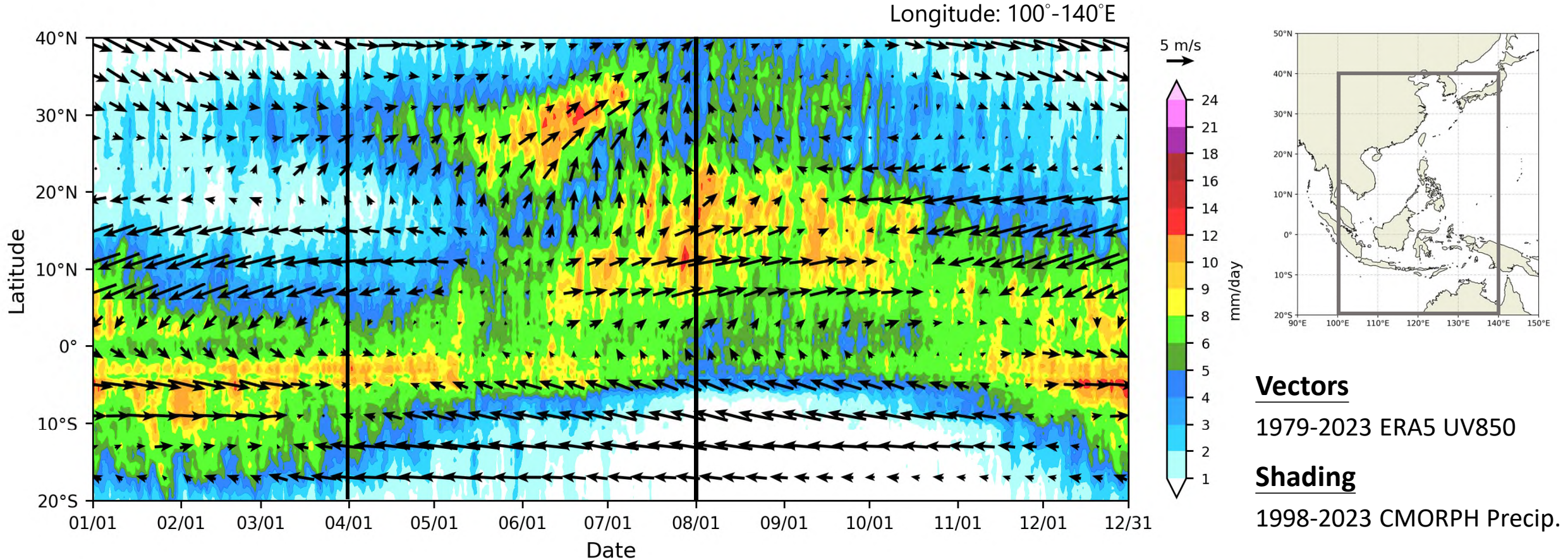


Vectors

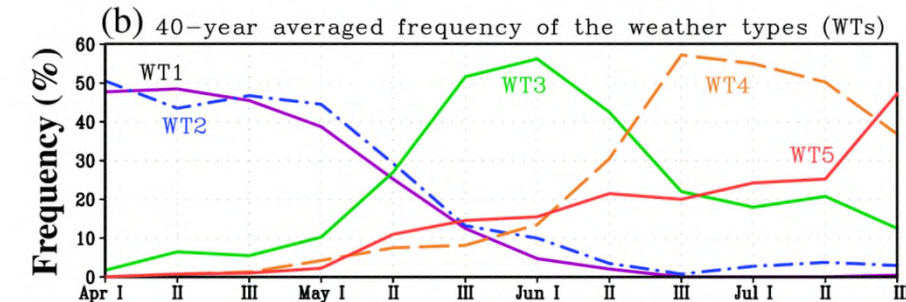
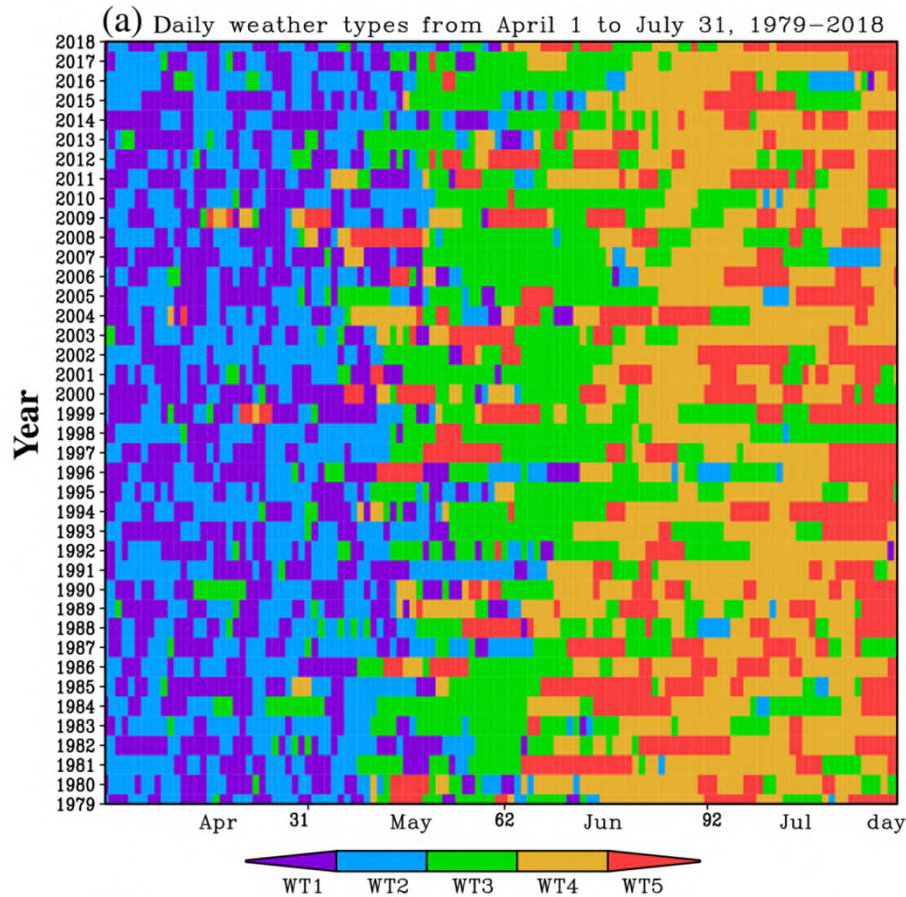
1979-2023 ERA5 UV850

Shading

1998-2023 CMORPH Precip.



- The transition of low-level wind from easterlies to westerlies during May to June coincides well with the precipitation from dry to wet condition.
- The low-level wind serves as an appropriate indicator for the monsoon evolution over East Asia.



- Qian et al. (2022) applied K-means clustering to analysis daily weather type over East Asia during April-July.

- ✓ Discuss climate in weather time scale
- ✓ Examine interannual climate variability

More detailed wind field patterns?
and seasonal evolution process?

- From another perspective, self-organizing map (SOM) method is adopted in this study for clustering analysis.

01 ○ Three Development Stages of EAM

To objectively separate the development stages of the EAM based on the AMJJ daily WTs.

02 ○ ENSO Modulations on EAM

To present the ENSO modulation on EAM climate variability using the EAM weather calendar.

03 ○ SOM WTs and Taiwan-Philippine Extreme Weather

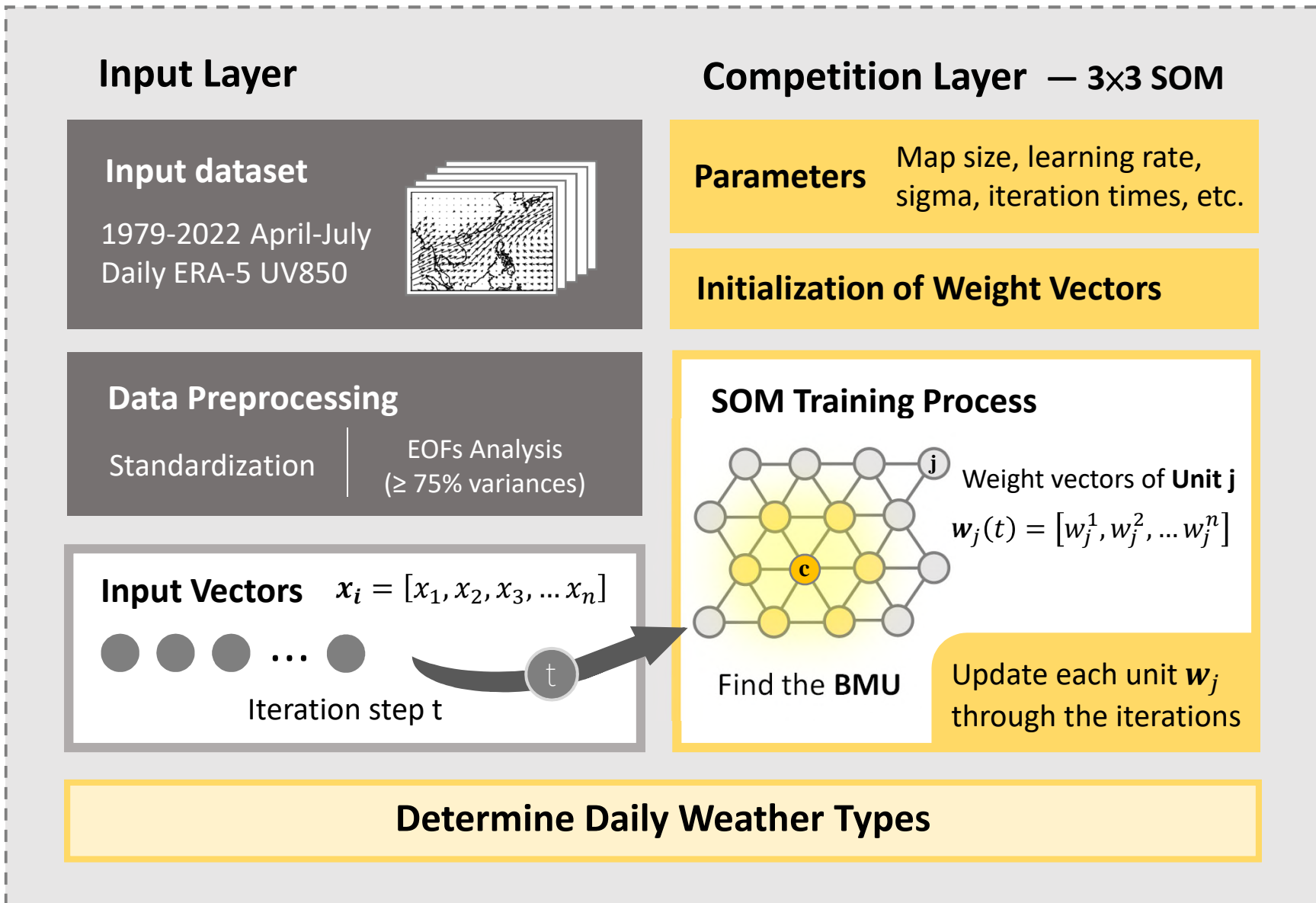
To investigate the extreme weather around Taiwan and Philippine regions through SOM WTs.

- **Research Domain:** the East-Asian monsoon region (0-37.5N, 90-140E) [Qian et al. 2022]

Dataset	Variables	Frequency	Grids	Periods
NOAA CMORPH	Precipitation	daily	0.25° × 0.25°	1998-2023 AMJJ
ECMWF ERA-5	UV850			1979-2023 AMJJ
	VIWV, VIWVD			
	Total Precipitation			
NOAA GPCP	Precipitation	pentad	2.5° × 2.5°	1979-2023 AMJJ
NOAA ERSST v5.	SST	monthly	2° × 2°	1951-2023
JMA RSMC Best Track Data (Including tropical cyclone of TD and TS intensity or higher)		6-hr	-	1979-2023 AMJJ

Weather Type Analysis – Self-organizing Maps (SOM)

Data and Methodology



Repeat Clustering

Random Seed = 1-300

Find the Most **Stable** and **Representative** Cases

Multi-SOM

67-case Clustering Results

Daily WTs

Combined-SOM

Spring-to-summer
Asian Monsoon Calendar

Naming WTs: Units A – I

ONI Calculation



OND

NDJ

DJF

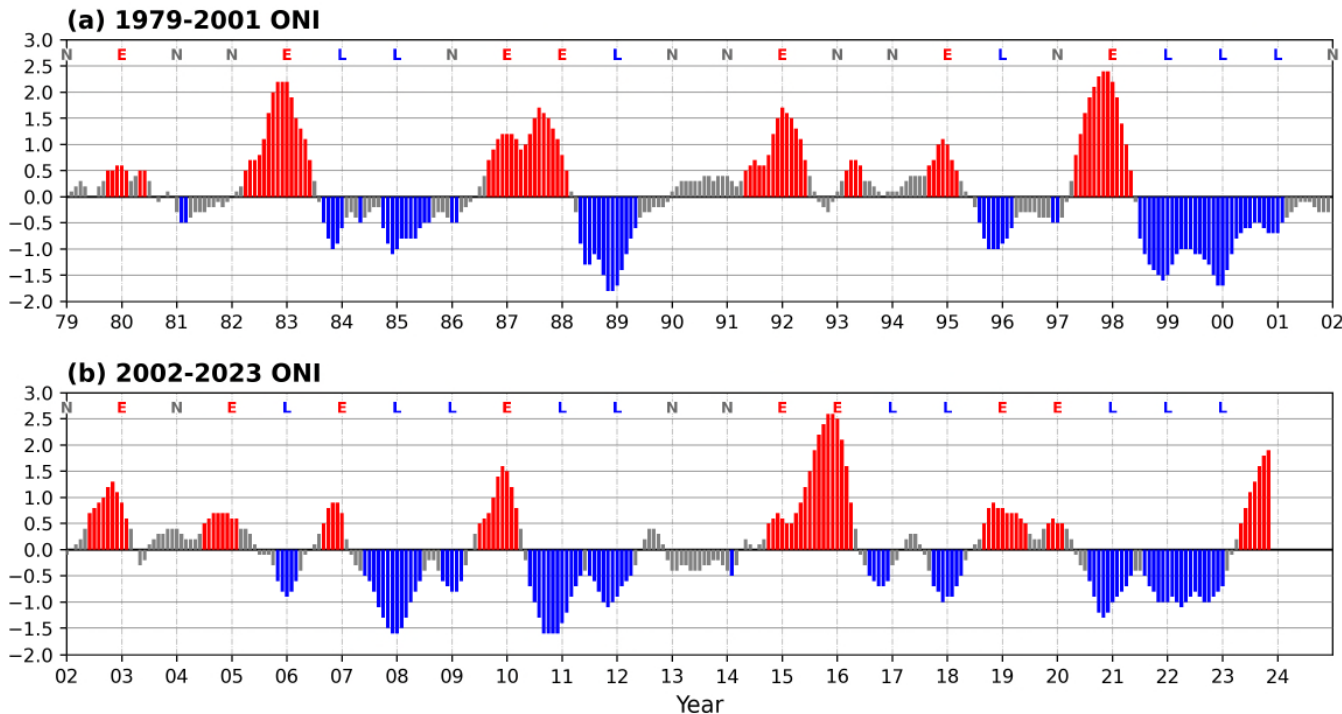
JFM

Data: NOAA ERSST v5

Region: Niño 3.4 (5N-5S, 120-170W)

(follow the definition of CPC)

Mean of any three ONI values > 0.5 **El Niño**
 < -0.5 **La Niña**



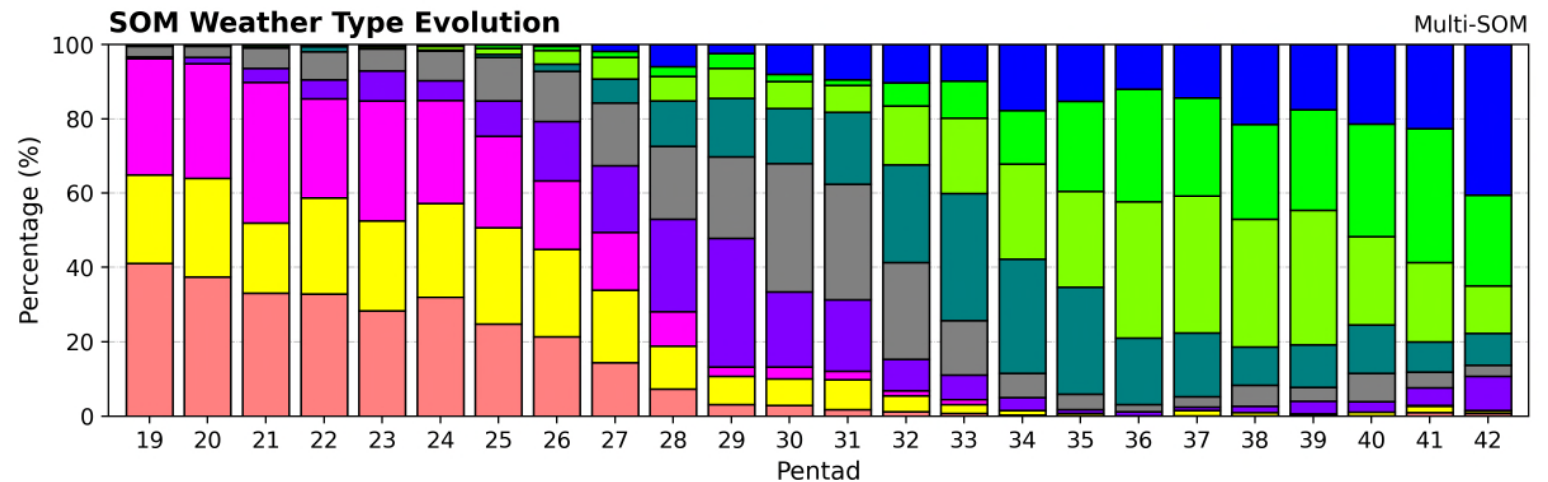
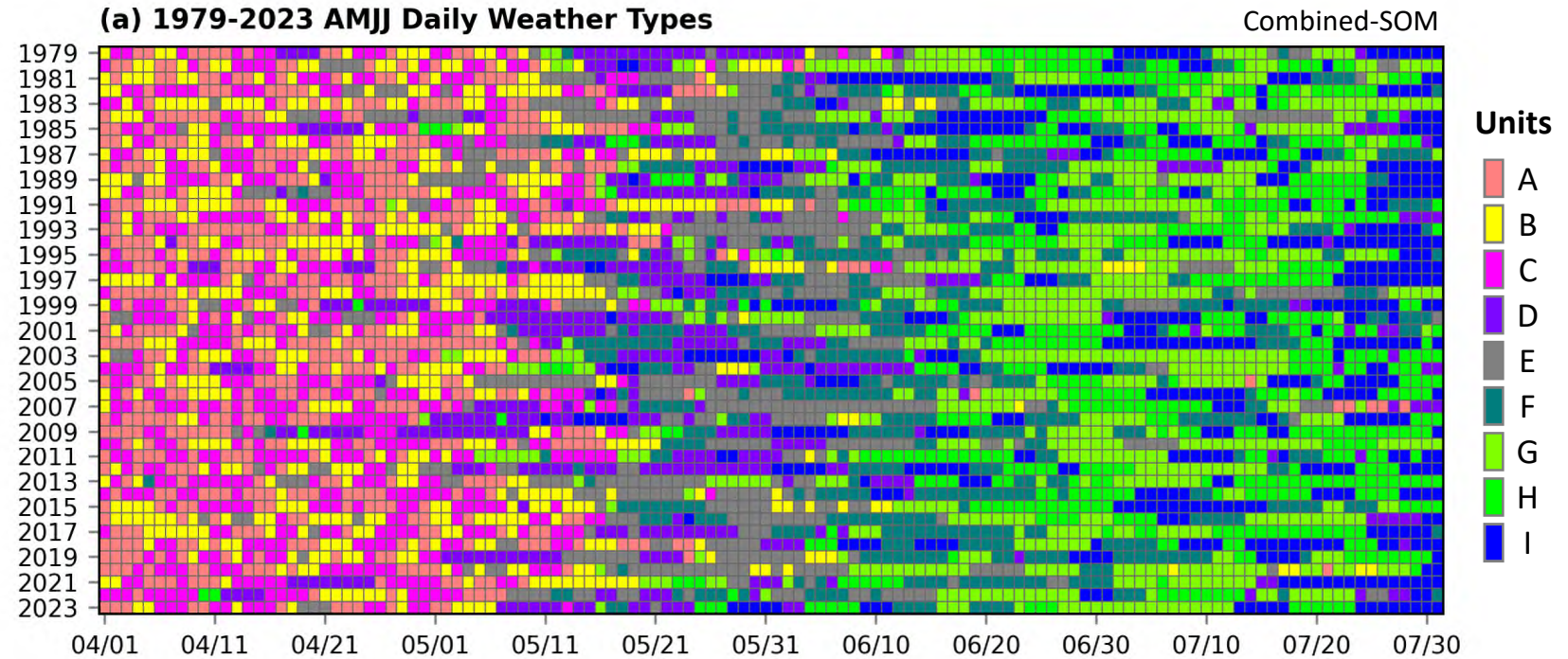
ENSO Phases	Years (1979-2023)
El Niño (15 yrs)	1980, 1983, 1987, 1988, 1992, 1995, 1998, 2003, 2005, 2007, 2010, 2015, 2016, 2019, 2020
Neutral (13 yrs)	1979, 1981, 1982, 1986, 1990, 1991, 1993, 1994, 1997, 2002, 2004, 2013, 2014
La Niña (17 yrs)	1984, 1985, 1989, 1996, 1999, 2000, 2001, 2006, 2008, 2009, 2011, 2012, 2017, 2018, 2021, 2022, 2023

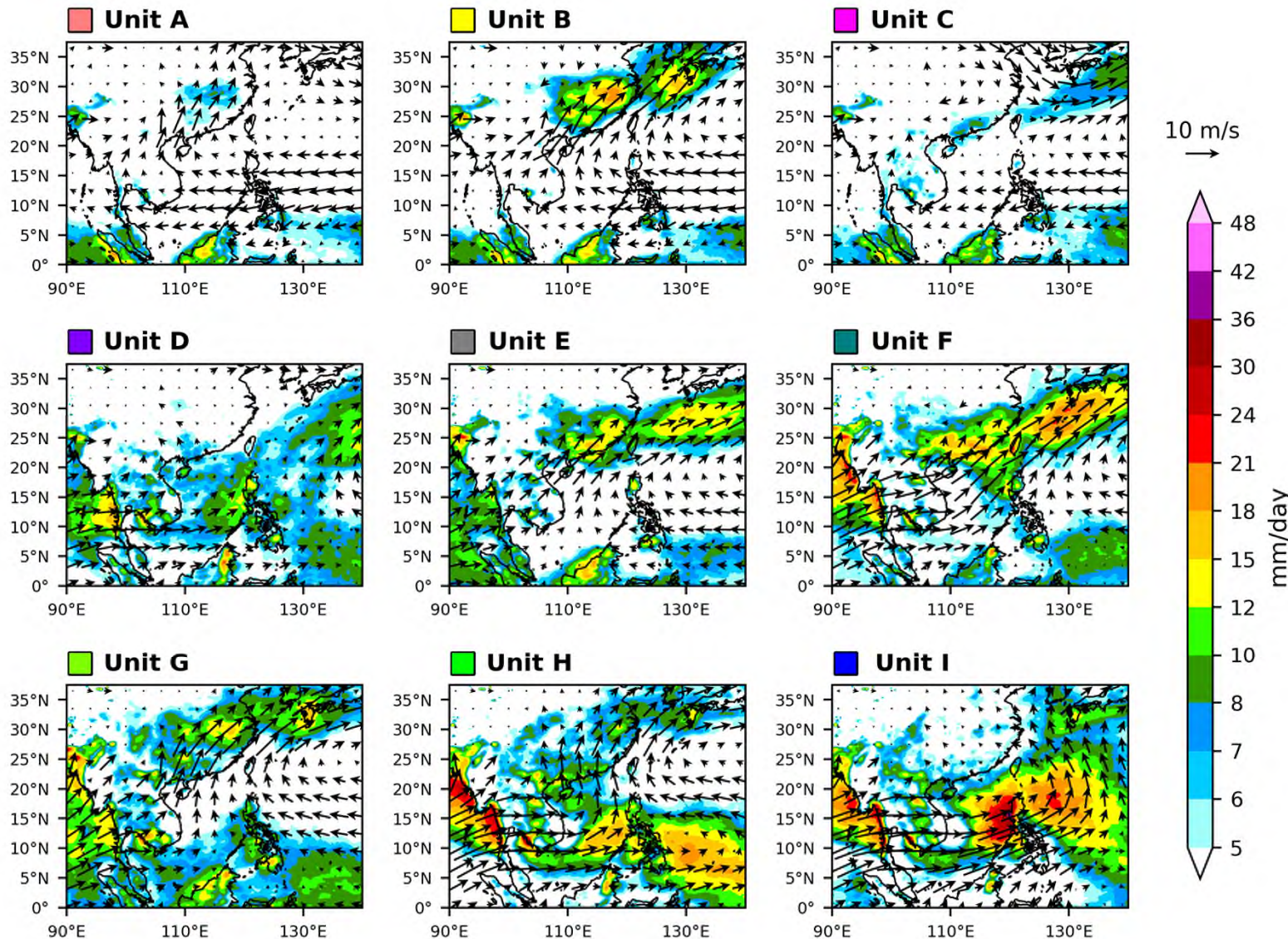
01

Three Development Stages of EAM

- SOM Weather Types
- EAM Weather Calendar
- Three Monsoonal Stages

- Seasonal evolution of EAM from April to July can be presented by the evolution of daily WTs.
- The period from early May to mid-June includes most kinds of WTs, illustrating the seasonal transition process.





Units A - C

- Strong easterlies over the SCS
- Weak precipitation over East Asia

Units D - F

- Westerlies from the BoB to SCS
- Precipitation contrast between E and F

Units G - I

- Northward movement of Mei-yu rainband
- Circulation of the subtropical high
- Monsoon trough

- Multi-SOM**



WTs occurrence on pentad time scale
 Arrange the WTs in chronological order

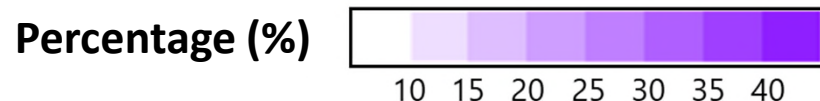
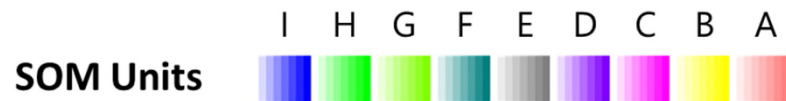
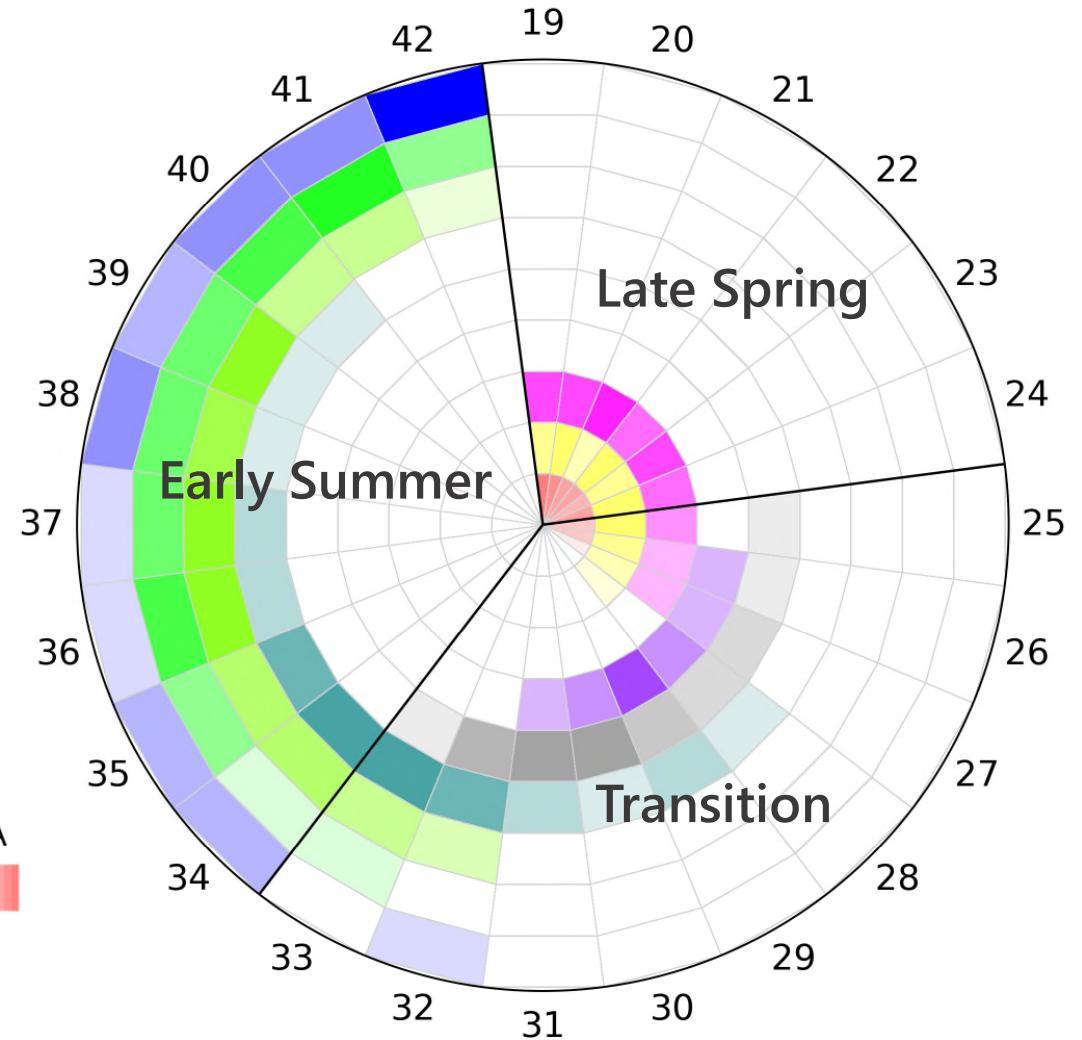
- EAM Weather Calendar**



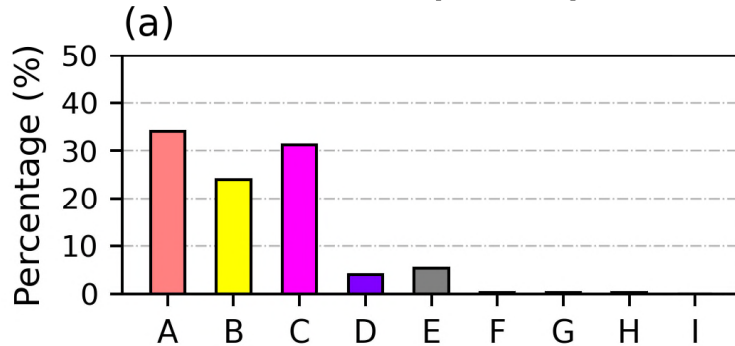
Dominant period of Unit E (the centered WT)
 Persisting occurrence of Unit I

- Three Development Stages of EAM**

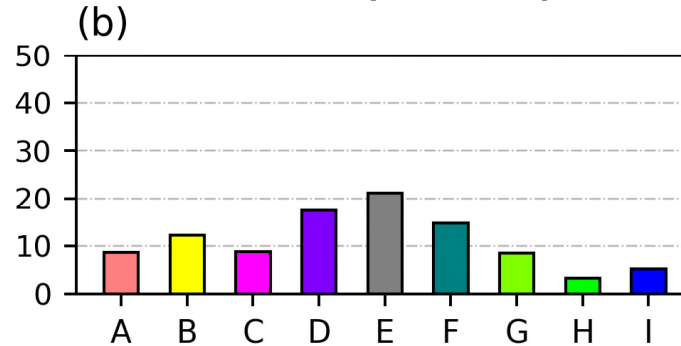
Pentad 19 (4/1-5) – Pentad 42 (7/25-29)



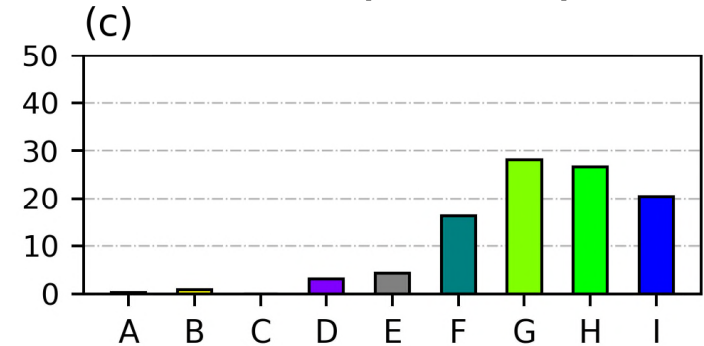
Late Spring
P19-24 (4/1-30)



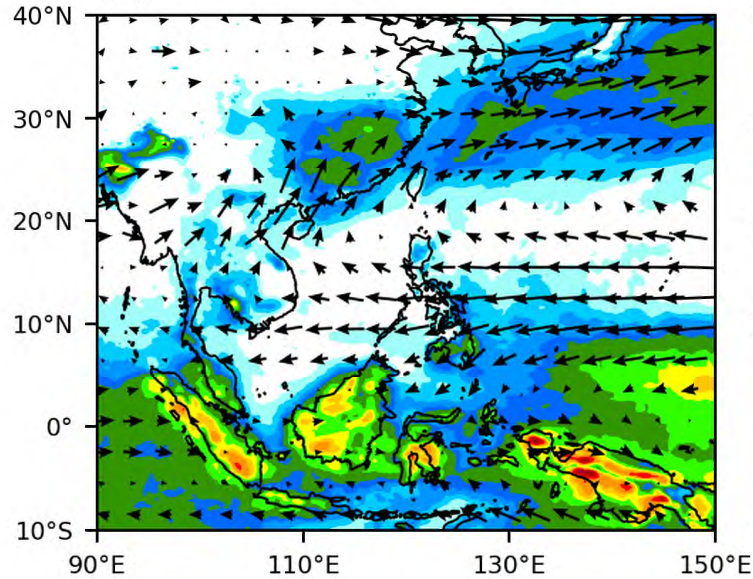
Transition
P25-33 (5/1-6/14)



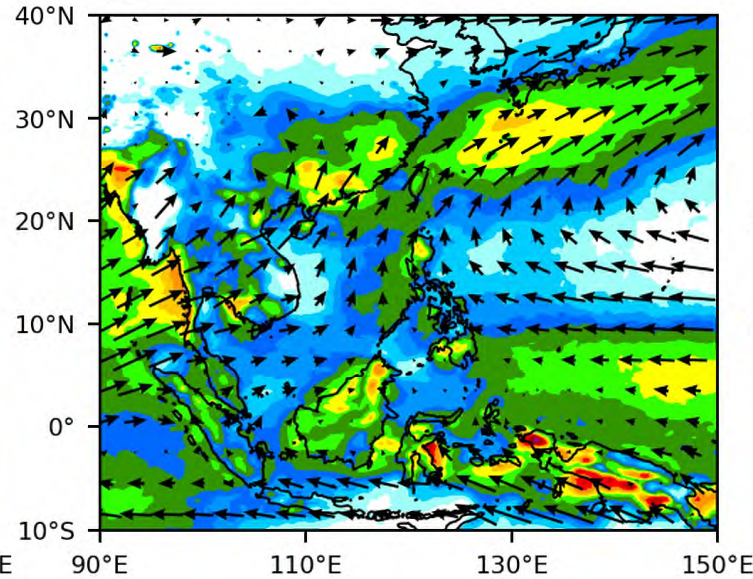
Early Summer
P34-42 (6/15-7/29)



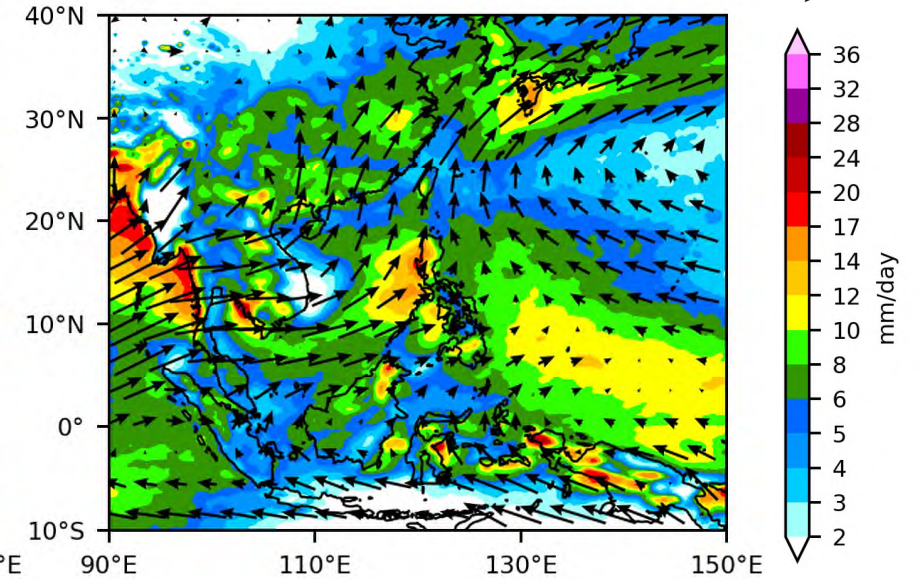
(d)



(e)



(f)



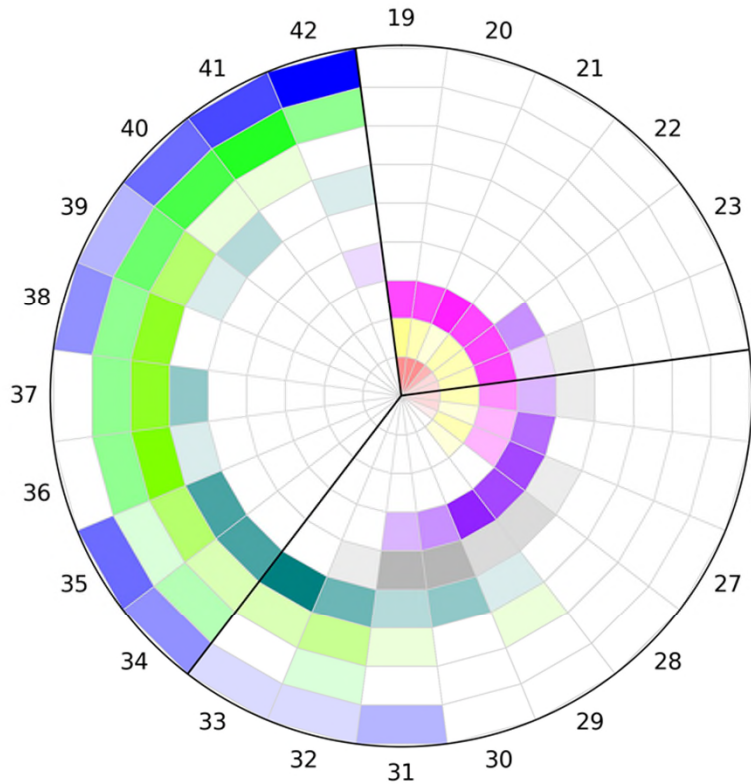
- The dominant WTs in three stages present the transition of climate regime from late spring to early summer.

02

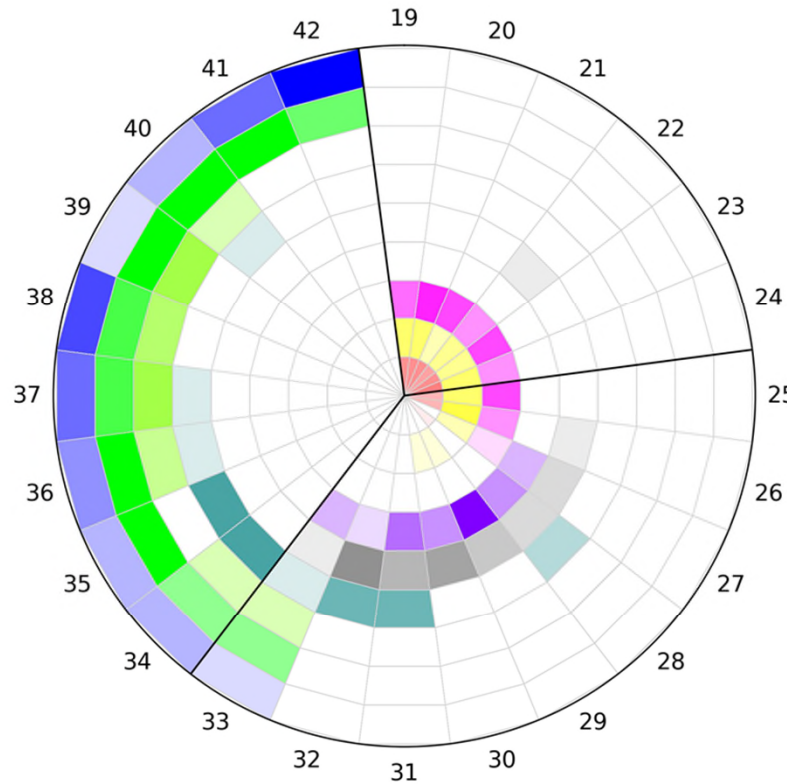
ENSO Modulations on EAM

- ENSO vs. SOM WTs
- ENSO Modulation

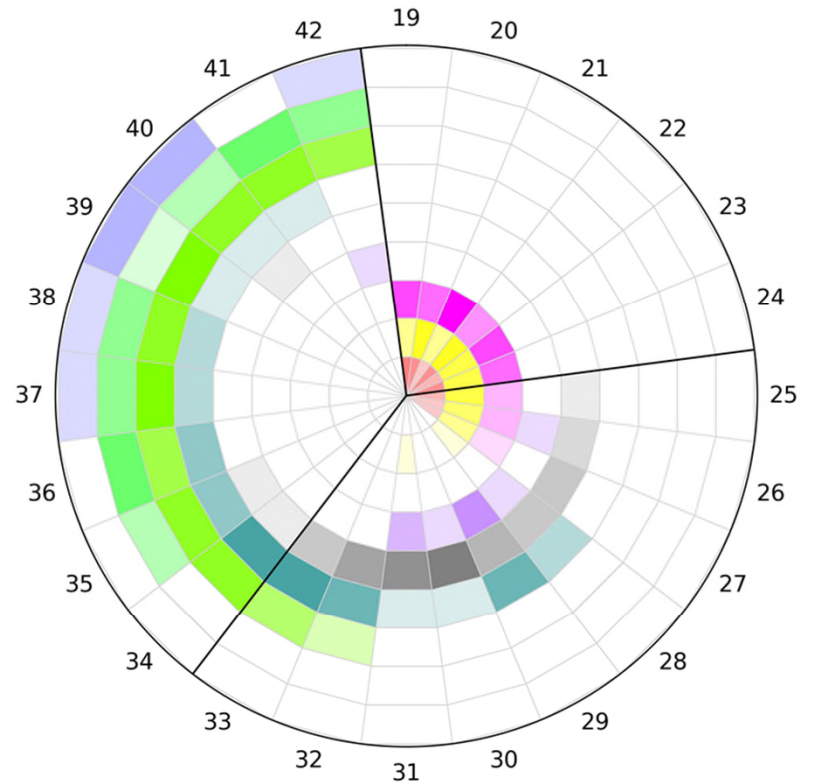
La Niña



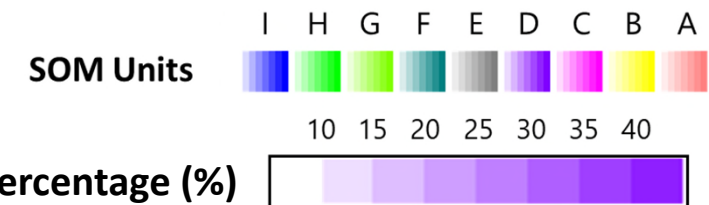
Neutral

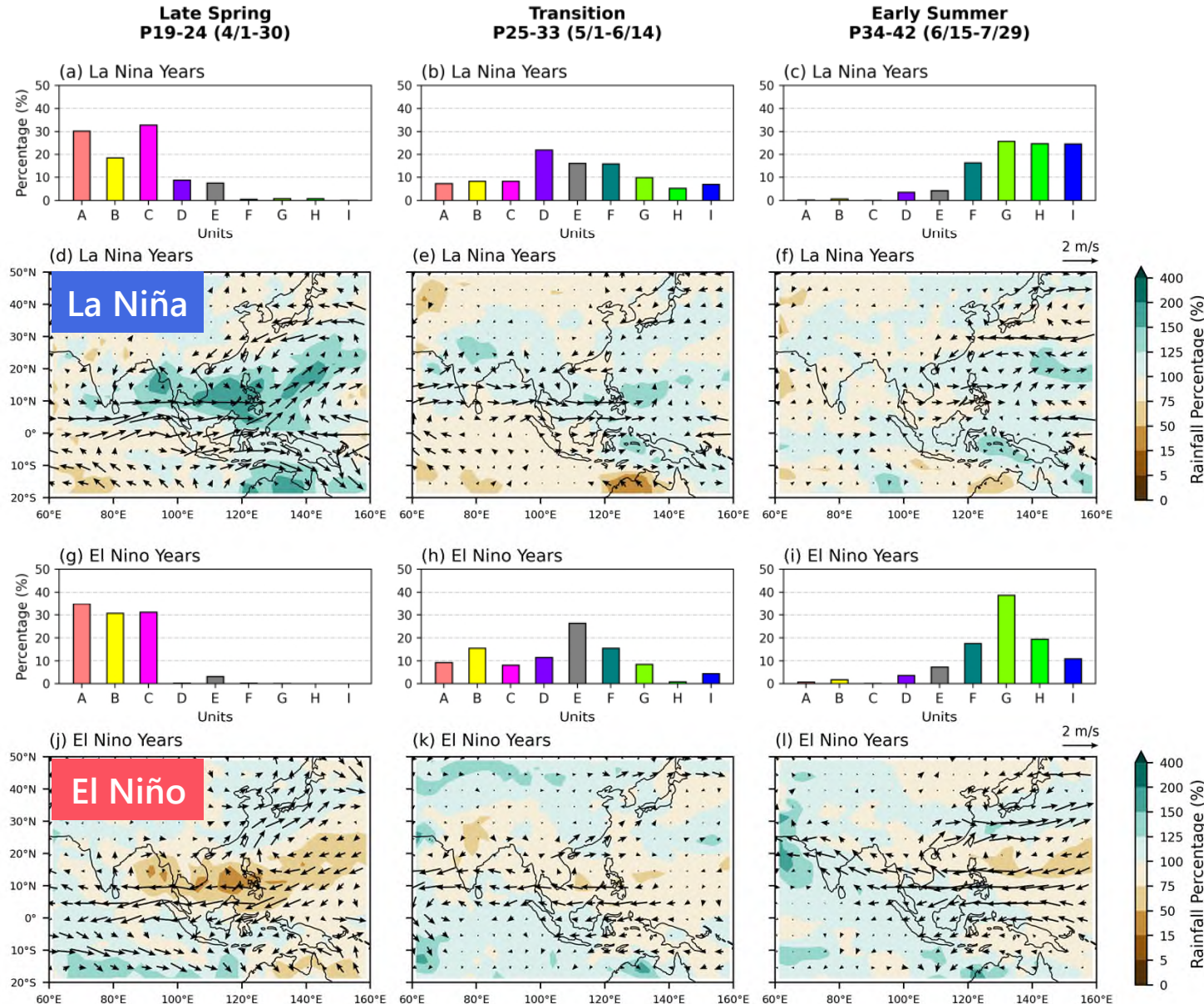


El Niño



- EAM weather calendars constructed by different ENSO years show different occurrence of WTs and their evolution processes.

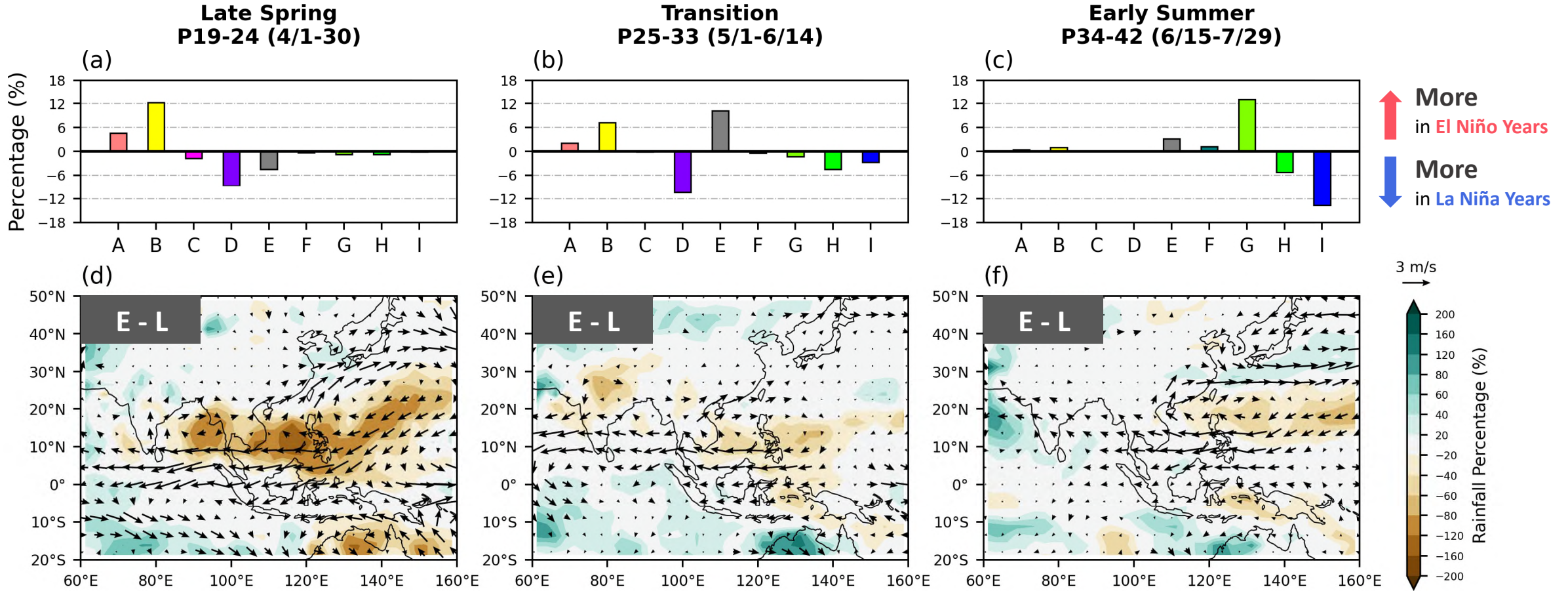




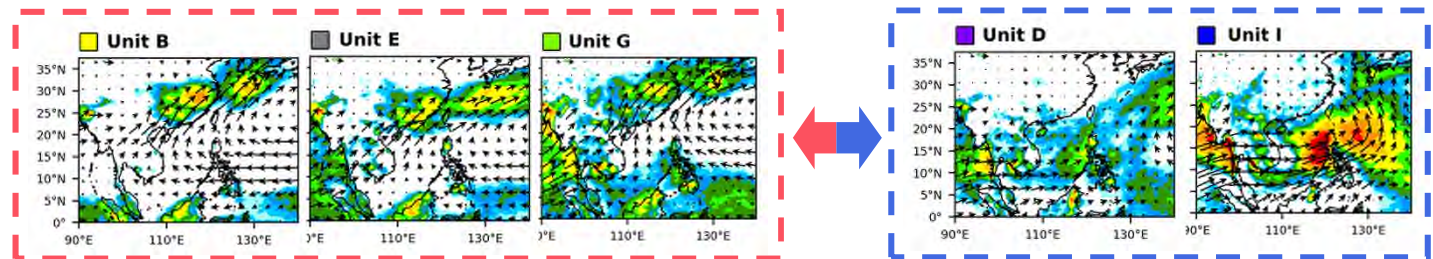
- The anticyclonic (cyclonic) anomalies and suppressed (enhanced) precipitation in El Niño (La Niña) years are shown in the composite maps.
- Different distribution of WTs reflect the anomalies of ENSO modulation in three monsoonal stages.

Vectors 1979-2023 ERA5 UV850

Shading 1979-2022 GPCP Rainfall pct.



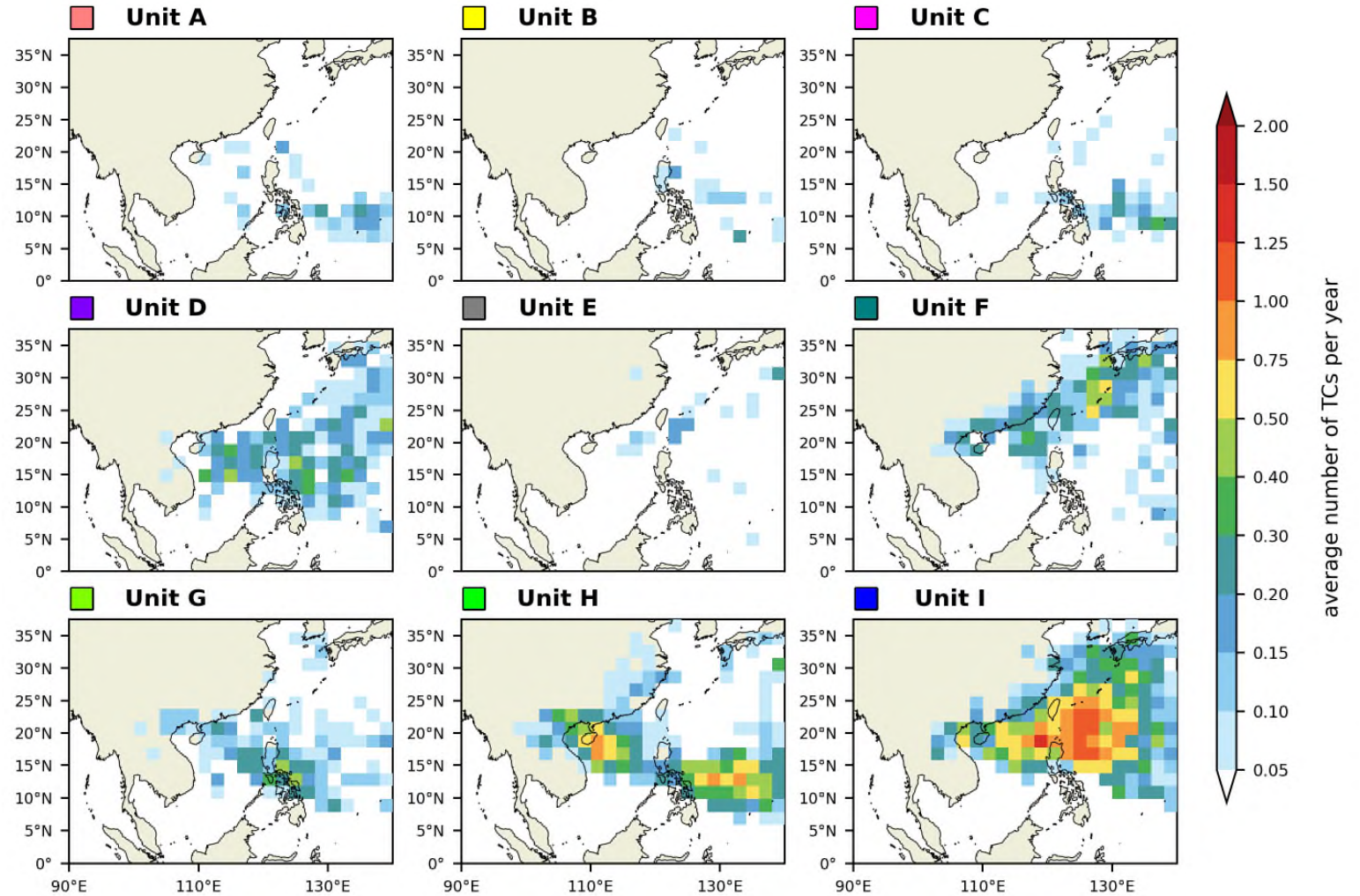
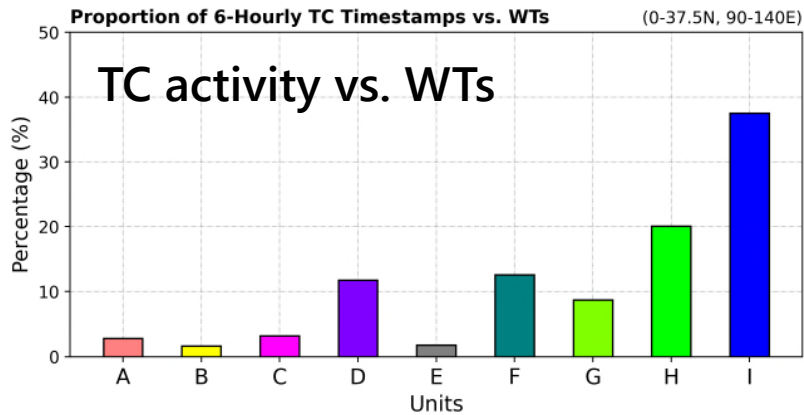
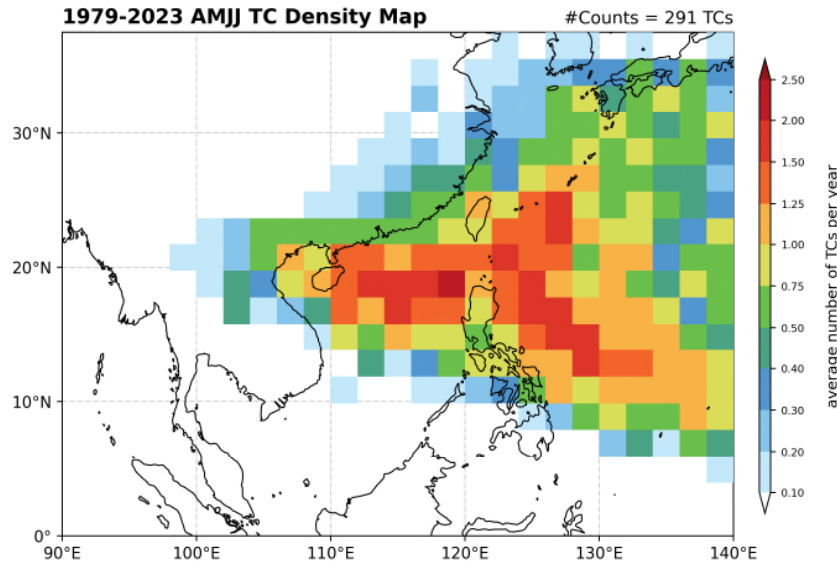
- Anticyclonic circulation over the WNP
- Easterlies from SCS to BoB
- Dry condition over the WNP



03

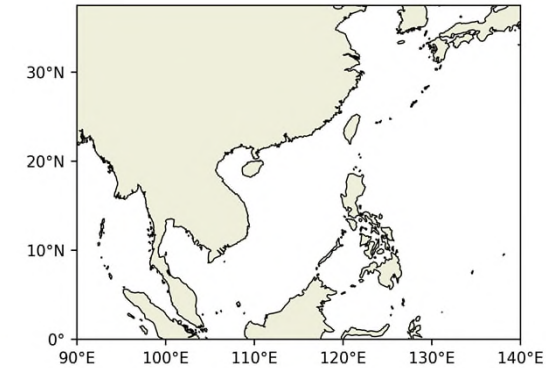
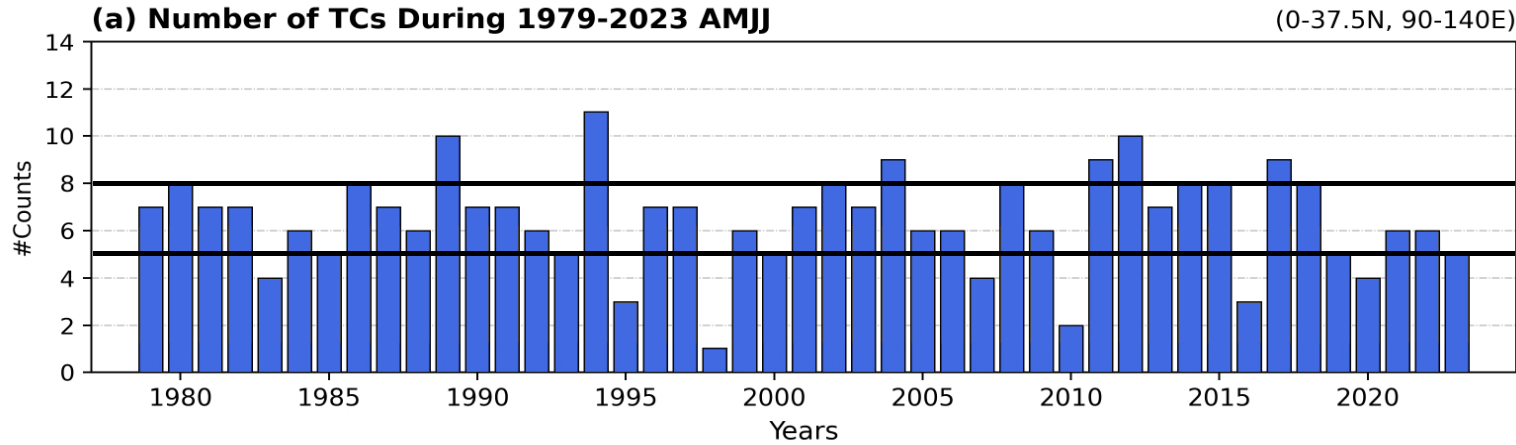
SOM WTs and Taiwan-Philippine Extreme Weather

- WNP TC Activity



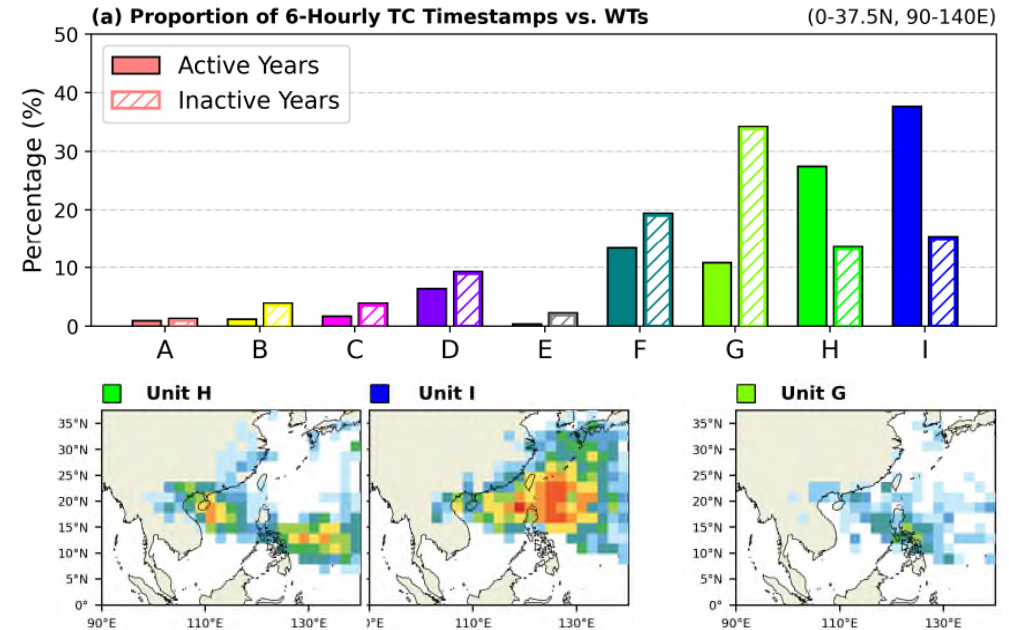
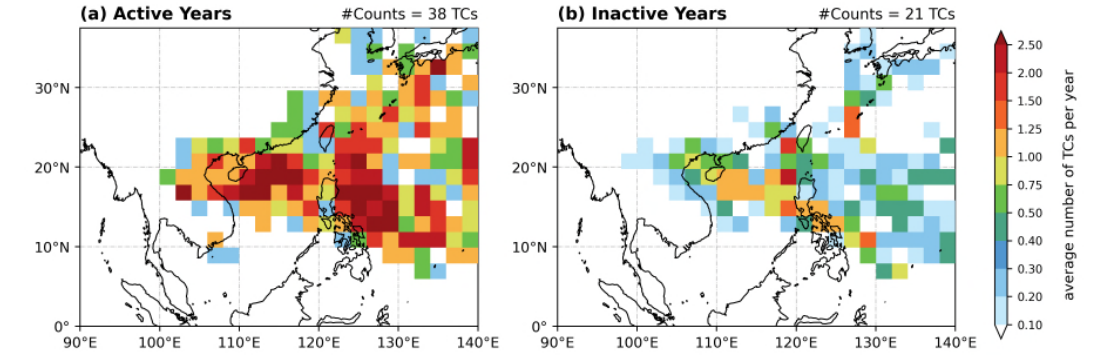
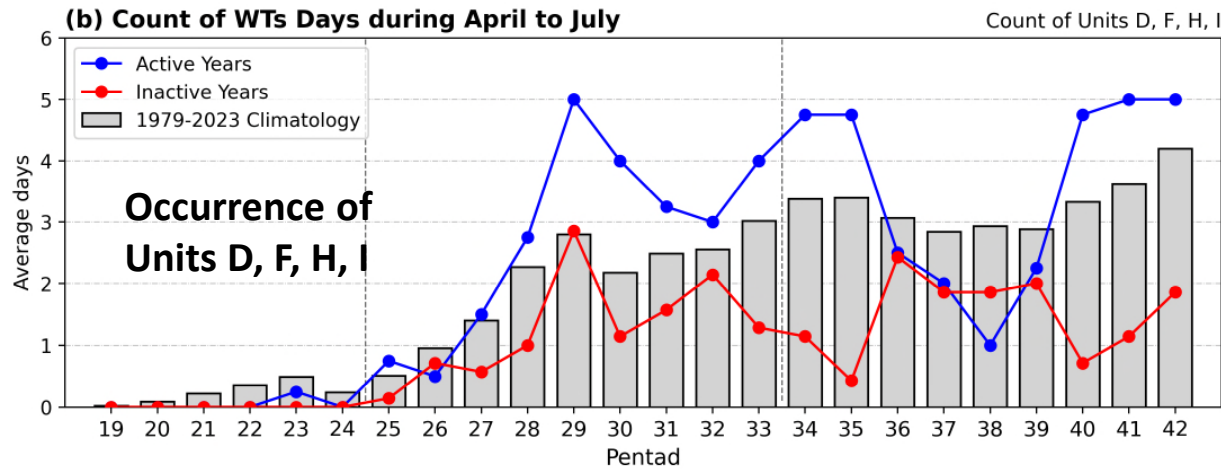
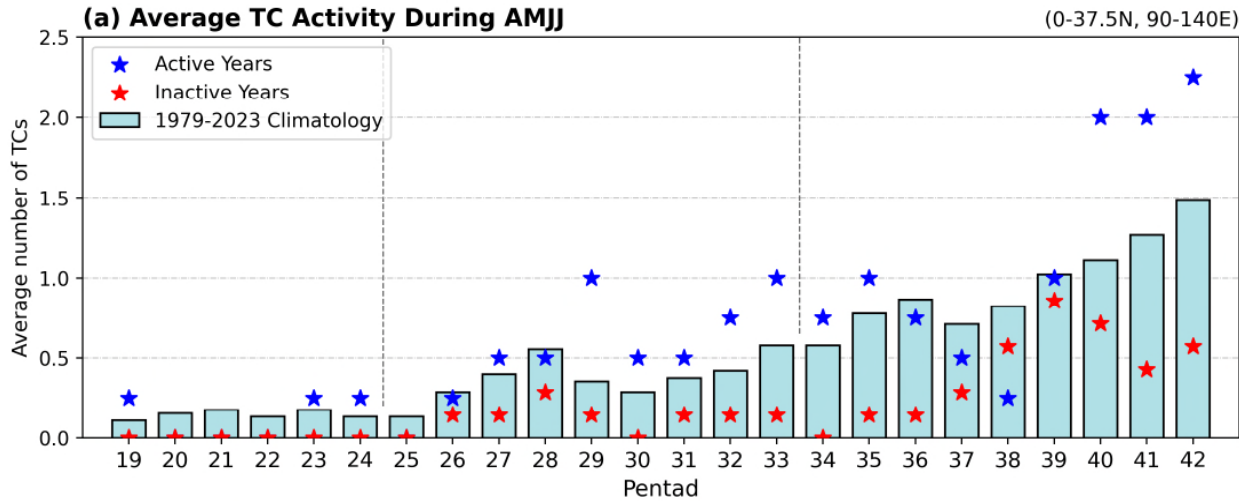
- Nine WTs show distinct spatial distribution and occurrence of TCs over the WNP.
- TC activity during April to July is primarily over the PhS and northern SCS, strongly related to Units H and I.

TC Activity during April to July vs. ENSO Phase



ENSO Phases	Number of TCs ≤ 4	$5 \leq$ Number of TCs ≤ 8	Number of TCs ≥ 9
El Niño	1983, 1995, 1998, 2007, 2010, 2016, 2020	1980, 1987, 1988, 1992, 2003, 2005, 2015, 2019	-
El Niño-inactive Years			
Neutral	-	1979, 1981, 1982, 1986, 1990, 1991, 1993, 1997, 2002, 2013, 2014	1994, 2004
La Niña-active Years			
La Niña	-	1984, 1985, 1996, 1999, 2000, 2001, 2006, 2008, 2009, 2018, 2021, 2022, 2023	1989, 2011, 2012, 2017

TC Activity and WTs of Active and Inactive Years



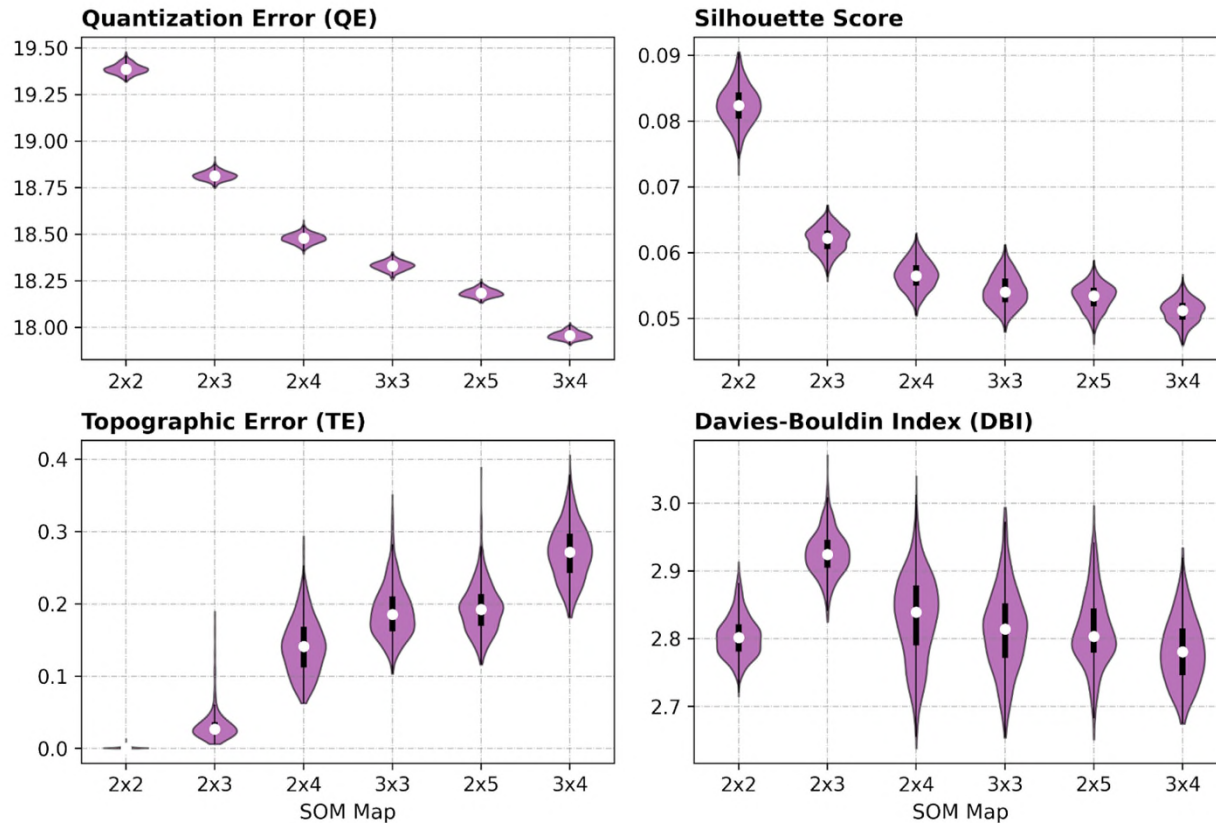
- The occurrence of WTs can properly reflect the TC activity over the WNP during April to July between La Nina-active and El Nino-inactive years.

Conclusions

- Three development stages of EAM during April to July are identified based on nine WTs of daily low-level wind data from 1979 to 2023 using SOM method, presenting on the EAM weather calendar.
- The ENSO modulation over East Asia on interannual time scale can be presented by different occurrence of WTs and the corresponding anomalous fields in three monsoonal stages.
- In the applications, the WTs and EAM weather calendar show that they can be used as a framework for monitoring or explaining the relationship between ENSO, EAM and TC activity over the WNP.

Future Works

- 擴大輸入資料的空間範圍，並嘗試延長分析時段（將以4-10月為主，涵蓋北半球主要降雨時期）。
- 嘗試應用此分析方法在即時氣候監測，以了解短期氣候的天氣類型演變特徵。
- 搭配其他客觀的分群評估指標，共同檢視 SOM 分群數量選擇的合理性。



重新使用500組 (seed=1-500) 不同群數的 SOM
對東亞4~7月逐日低層風場的分群結果評估

- Cho, Y., and M. Lu, 2021: Taiwan Mei-yu seasonal rainfall pattern and East Asian Summer Monsoon characteristics during the monsoon development stage. *Atmospheric Sciences*, **49**, 79-109.
- Clark, S., S. A. Sisson, and A. Sharma, 2020: Tools for enhancing the application of self-organizing maps in water resources research and engineering. *Adv. Water Resour.*, **143**, 16.
- Dai, L., T. F. Cheng, and M. Q. Lu, 2021: Define East Asian Monsoon Annual Cycle via a Self-Organizing Map-Based Approach. *Geophys. Res. Lett.*, **48**, 12.
- Ding, Y., and J. Chan, 2005: The East Asian summer monsoon: an overview. *Meteorol. Atmos. Phys.*, **89**, 117-142.
- Huang, W. Y., R. Y. Chen, Z. F. Yang, B. Wang, and W. Q. Ma, 2017: Exploring the combined effects of the Arctic Oscillation and ENSO on the wintertime climate over East Asia using self-organizing maps. *J. Geophys. Res.-Atmos.*, **122**, 9107-9129.
- Kohonen, T., 1990: THE SELF-ORGANIZING MAP. *Proc. IEEE*, **78**, 1464-1480.
- Nishiyama, K., S. Endo, K. Jinno, C. B. Uvo, J. Olsson, and R. Berndtsson, 2007: Identification of typical synoptic patterns causing heavy rainfall in the rainy season in Japan by a Self-Organizing Map. *Atmos. Res.*, **83**, 185-200.
- Qian, J. H., M. M. Lu, and C. H. Sui, 2022: Evolution of South China Sea and East Asian monsoon from spring to summer by the progression of daily weather types. *Int. J. Climatol.*, **42**, 3633-3647.
- Wang, B., and Q. Zhang, 2002: Pacific-east Asian teleconnection. Part II: How the Philippine Sea anomalous anticyclone is established during El Nino development. *J. Climate*, **15**, 3252-3265.
- Wang, B., and J. C. L. Chan, 2002: How Strong ENSO Events Affect Tropical Storm Activity over the Western North Pacific. *J. Climate*, **15**, 1643-1658.
- Wang, B., R. G. Wu, and X. H. Fu, 2000: Pacific-East Asian teleconnection: how does ENSO affect East Asian climate? *J. Climate*, **13**, 1517-1536.
- Wang, B., R. Wu, and T. Li, 2003: Atmosphere–warm ocean interaction and its impacts on Asian–Australian monsoon variation. *J. Climate*, **16**, 1195-1211.
- Xie, S. P., K. M. Hu, J. Hafner, H. Tokinaga, Y. Du, G. Huang, and T. Sampe, 2009: Indian Ocean Capacitor Effect on Indo-Western Pacific Climate during the Summer following El Nino. *J. Climate*, **22**, 730-747.

Quantization Error (QE) **Lower is better**

QE is the average distance between data points and their corresponding best-matching units (BMUs) on the map.

$$QE = \frac{1}{N} \sum_{i=1}^N \|w_c - x_i\|$$

N : number of input samples
 x_i : input vector of sample i
 c : Best matching unit of sample i
 w_c : weight vector of Unit c

Topographic Error (TE) **Lower is better**

TE measures the degree of topology preservation, which indicate whether similar clusters are positioned closely on the map.

$$TE = \frac{1}{N} \sum_{i=1}^N u_{x_i}$$

$$u_{x_i} = \begin{cases} 0, & \text{if 1}^{\text{st}} \text{ and 2}^{\text{nd}} \text{ BMU of } x_i \text{ are neighbors} \\ 1, & \text{if 1}^{\text{st}} \text{ and 2}^{\text{nd}} \text{ BMU of } x_i \text{ are not neighbors} \end{cases}$$

Silhouette Score 輪廓係數 **Higher is better**

The silhouette score is to measure each data point's similarity to the cluster it belongs to and how different it is from other clusters.

$$s(i) = \frac{b(i) - a(i)}{\max\{a(i), b(i)\}} \quad \begin{cases} s(i) \approx 1 : \text{Well-clustered.} \\ s(i) \approx 0 : \text{Between two clusters.} \\ s(i) < 0 : \text{Likely misclassified.} \end{cases}$$

$s(i)$: silhouette score of sample i

$a(i)$: Avg. distance to points in the same cluster

$b(i)$: Avg. distance to points in the nearest different cluster

Davies-Bouldin Index (DBI) **Lower is better**

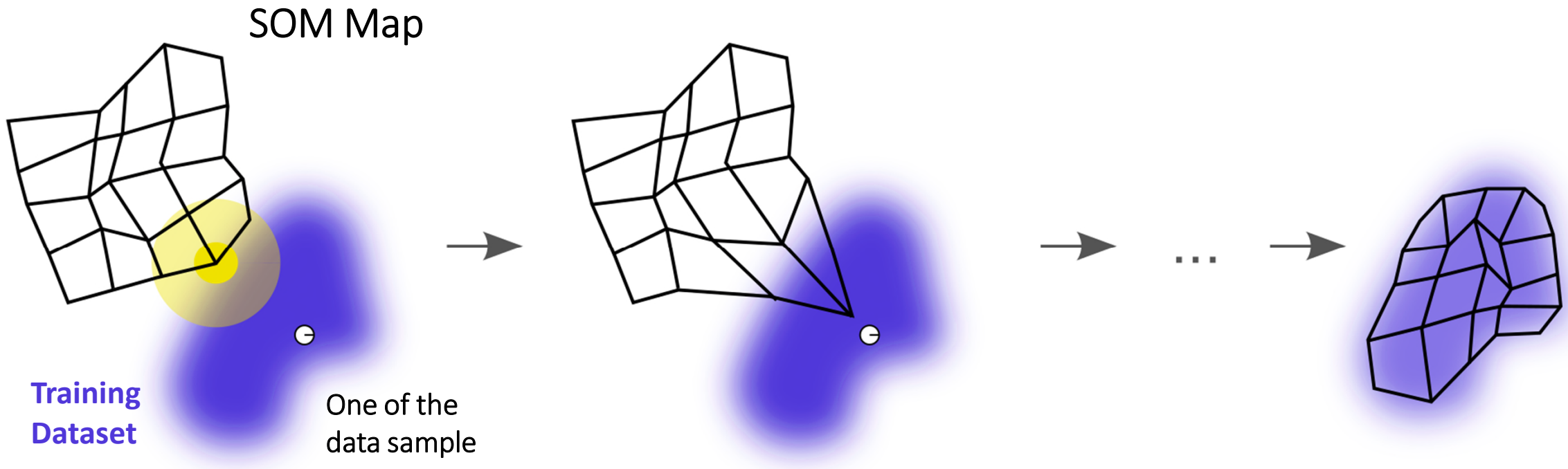
DBI measures how good clusters are by checking if the points in each cluster are close together (compactness) and if the clusters are far apart from each other (separation).

$$DBI = \frac{1}{k} \sum_{i=1}^k \max_{j \neq i} \left(\frac{S_i + S_j}{M_{ij}} \right)$$

k : Number of clusters

S_i : Avg. distance of points in cluster i to its center

M_{ij} : Distance between centers of clusters i and j



- The ENSO modulation on the interannual variability of EAM are well documented in previous studies. [Wang and Zhang 2002; Wang et al. 2000; Wang et al. 2003; Xie et al. 2009]
- The delayed impact of ENSO on the SCS and Philippine Sea region is related to anomalous Philippine Sea anticyclone, persisting from mature El Nino to ensuing summer. [Wang and Zhang 2002; Wang et al. 2000]

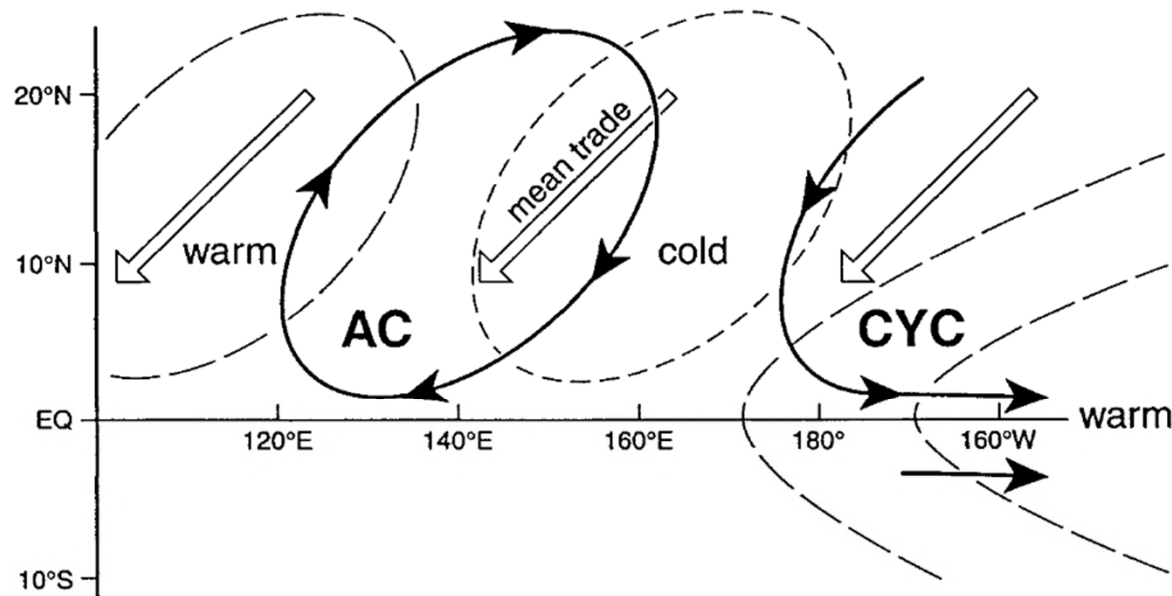
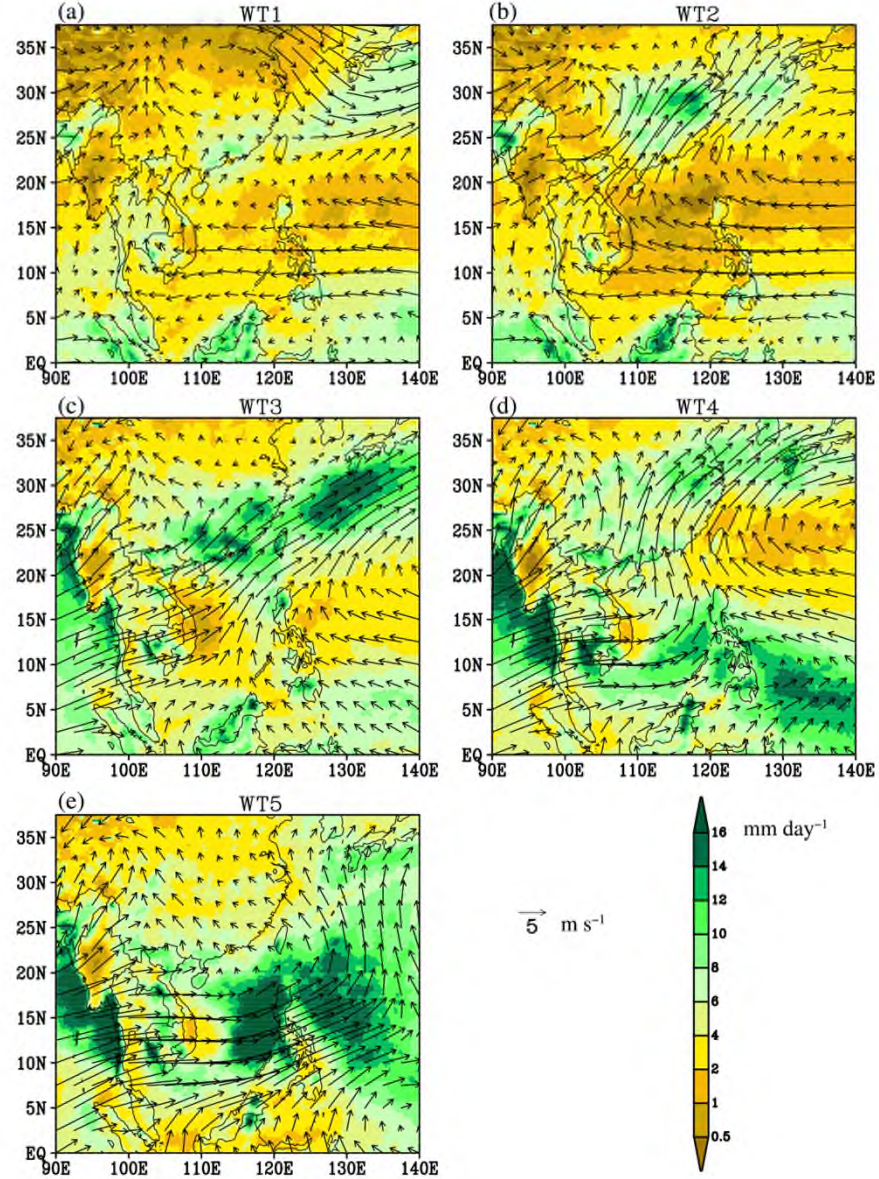
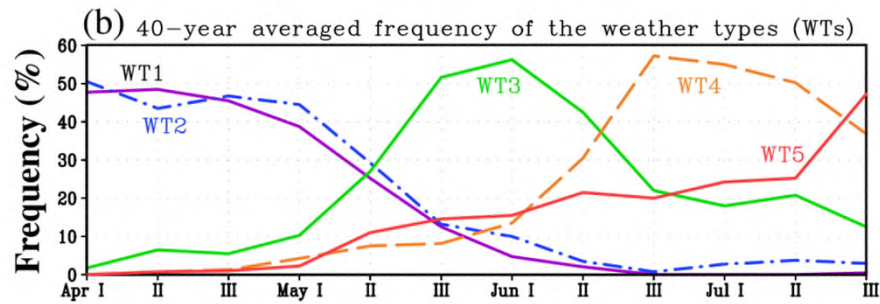
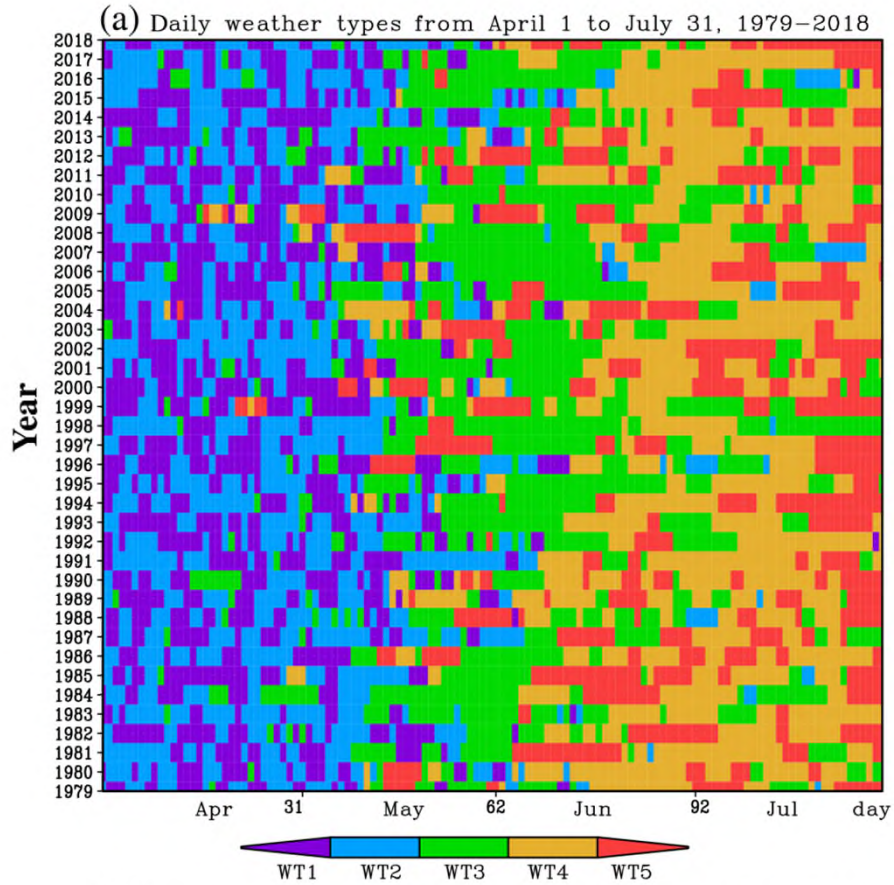
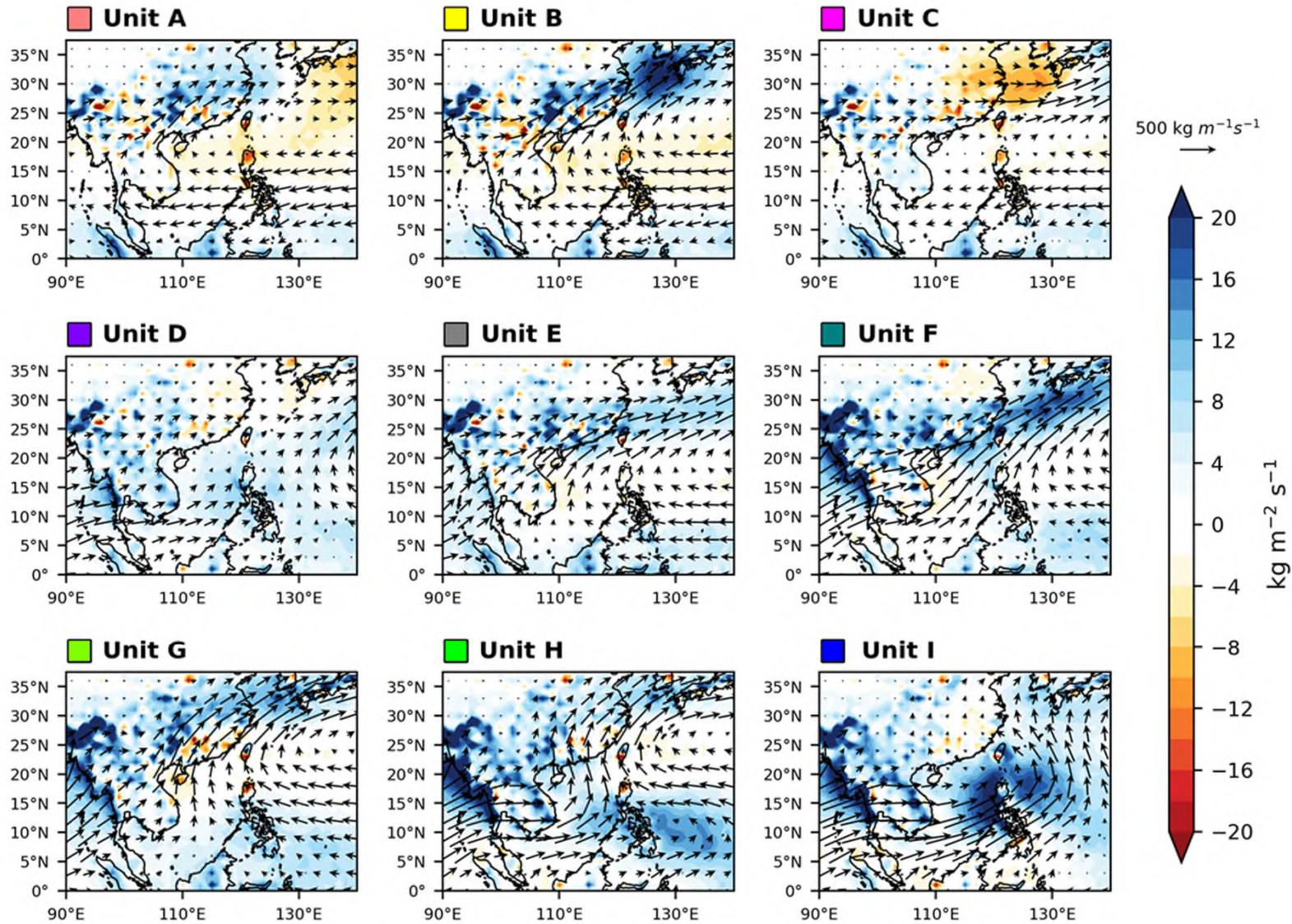


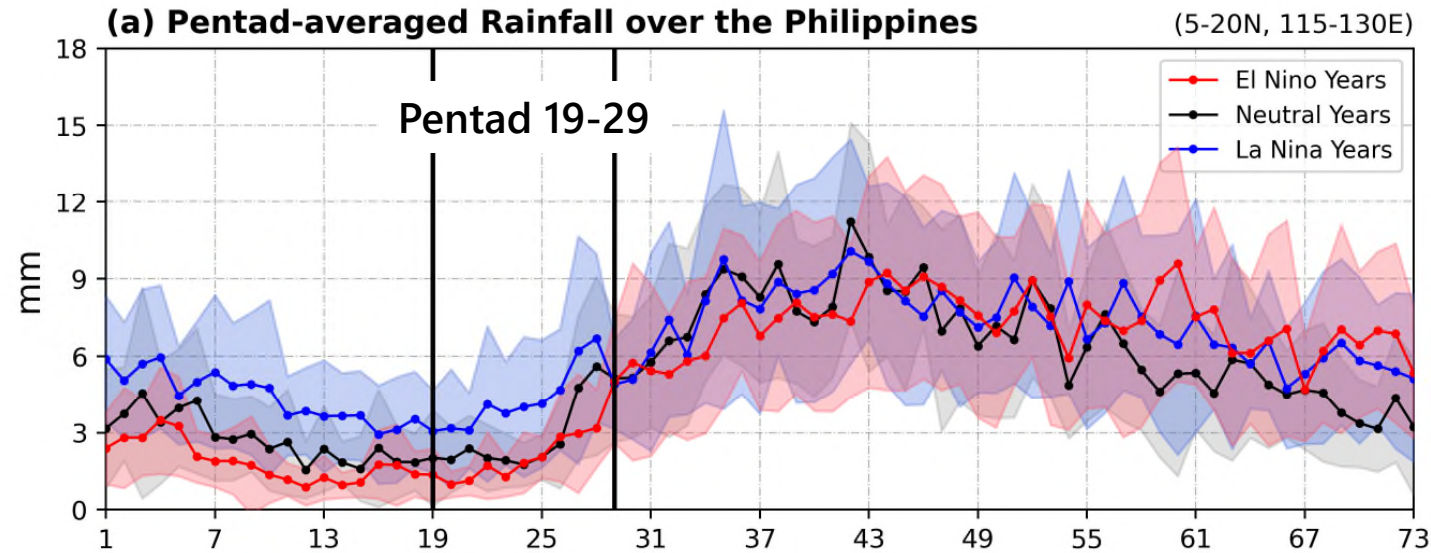
FIG. 16. Schematic diagram showing the air-sea interaction in the western North Pacific that maintains the Philippine Sea anticyclonic anomalies and associated negative SST anomalies in the western North Pacific. The double arrows denote the mean trade winds. The heavy lines with black arrows represent the anomalous winds. The long (short) dashed lines indicate contours of positive (negative) SST anomalies.

Wang et al. 2000

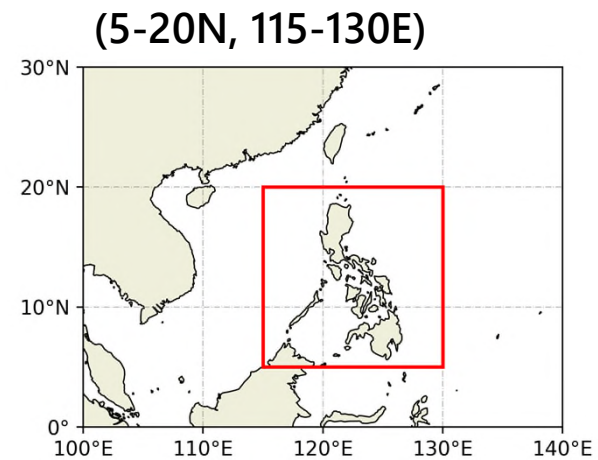
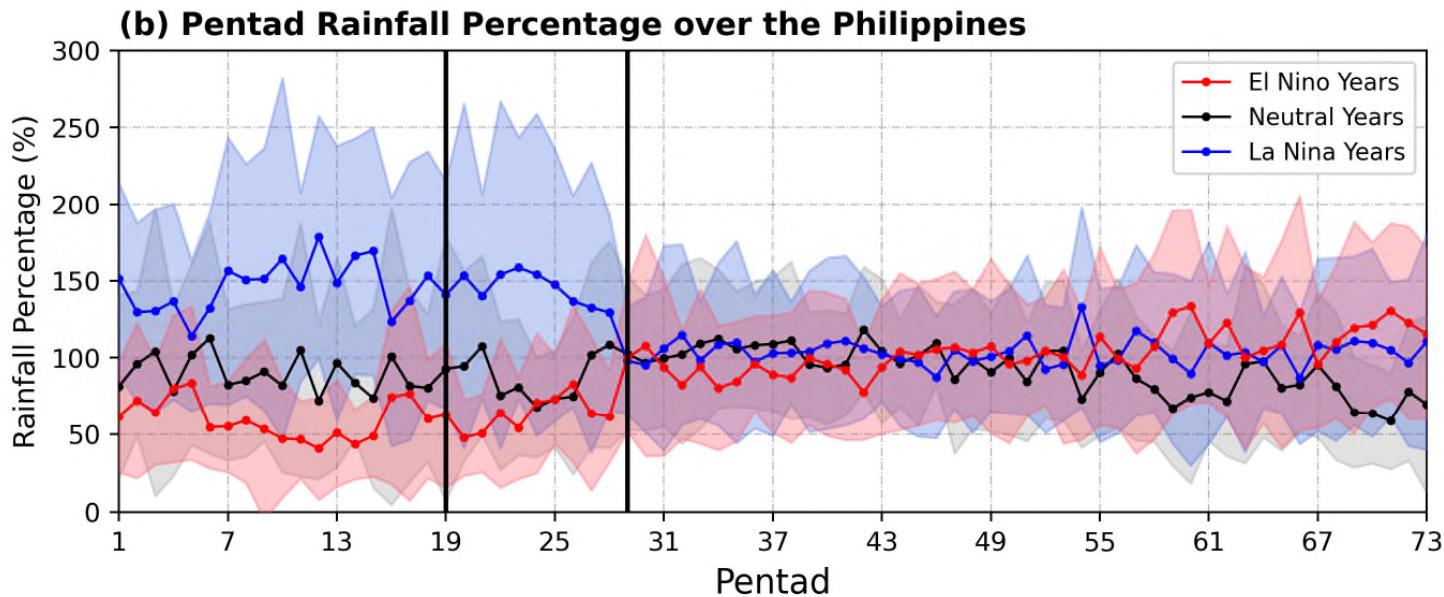




- The vertically-integrated water vapor transport and flux convergence shows the consistent features with low-level wind and precipitation fields.

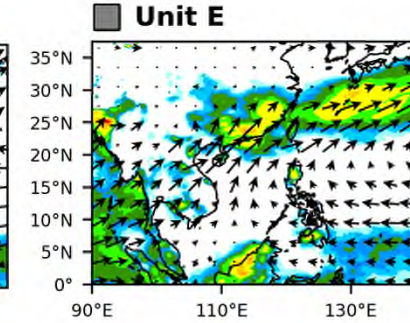
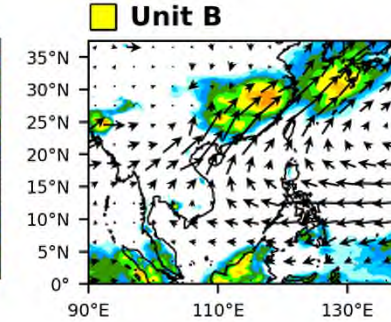
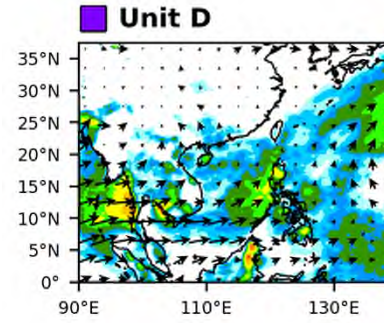
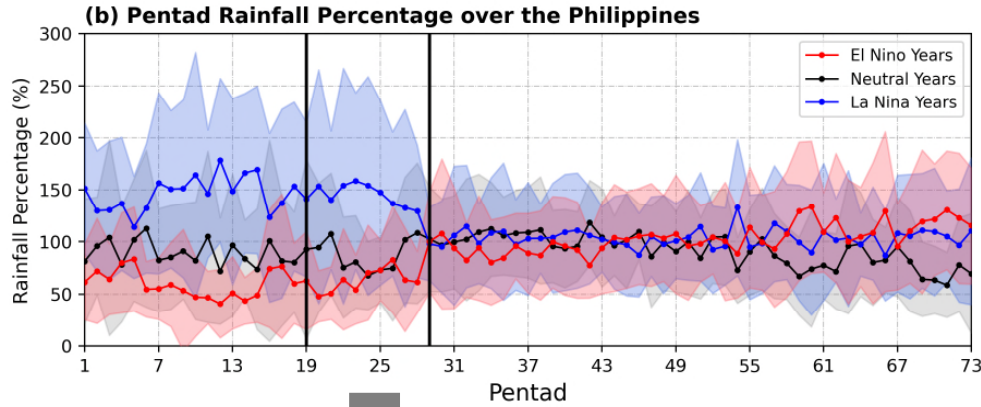


- More rainfall in La Niña years.
- Less rainfall in El Niño years.
- ENSO modulation on rainfall over the Philippines is from winter time to pre-rainy season, while no clear differences after Pentad 29 (5/21-25).

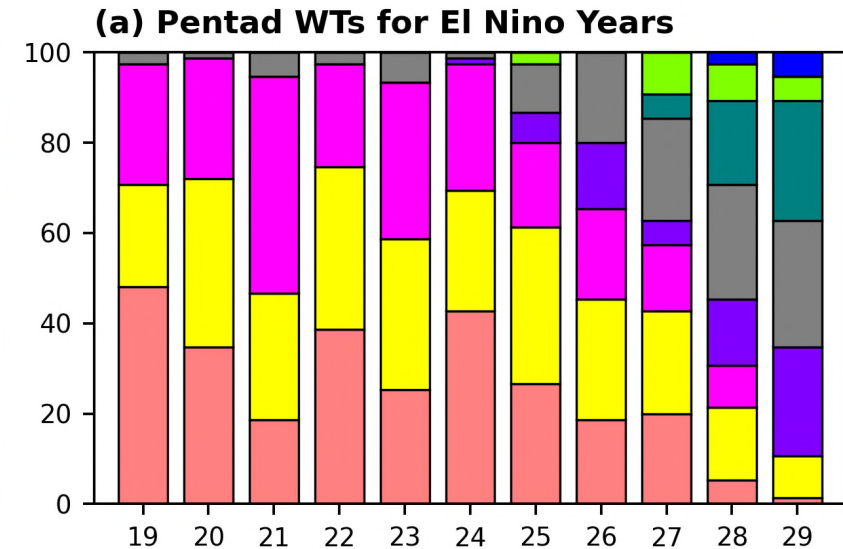
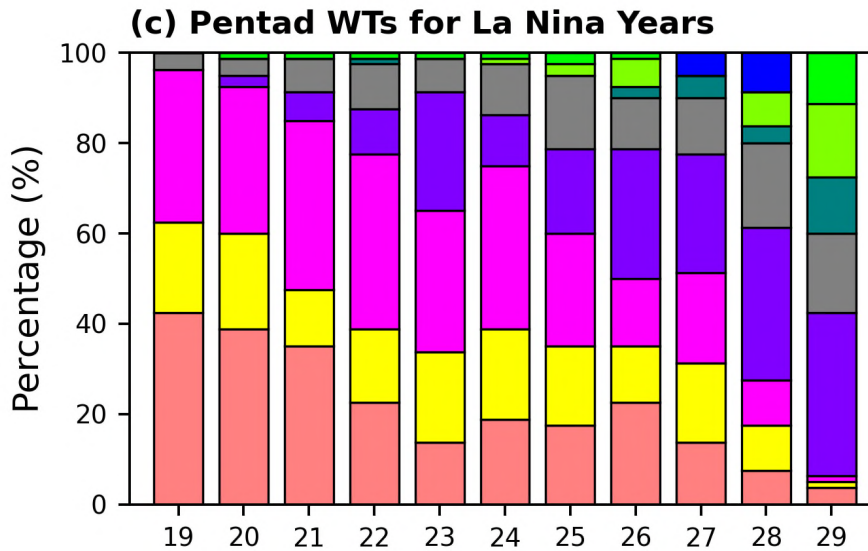


WT Occurrence during Philippine Pre-rainy Season

Philippine Pre-rainy Season



SOM WTs
During P19-29



- The contrast of pre-rainy season over the Philippines between La Niña and El Niño years can be reflected by the different occurrence of Units B, E, D.

Extreme Rainfall Analysis

ERA-5 Total Precipitation

- Grids: $2.5^\circ \times 2.5^\circ$
- Time: 1979-2023 4/26-7/4

Calculate Rainfall Thresholds

- Dry day: Below PR10
- Wet day: Exceed PR90

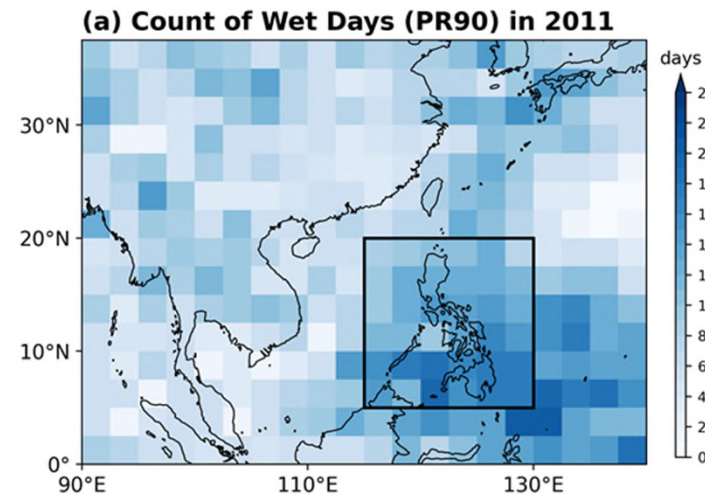
Dry/Wet Days for Selected Regions

Count the dry/wet days for each grid, averaged over Taiwan and the Philippines.

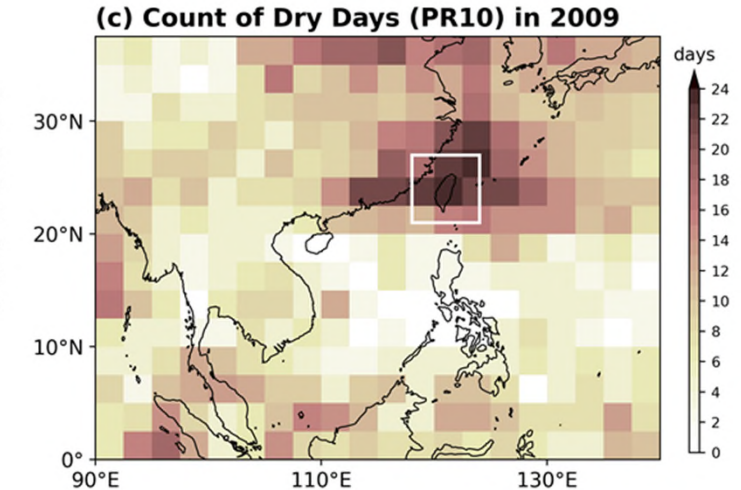
Compare with ENSO

Corr.	PHL	TW
Dry days vs. DJF ONI	0.56***	-0.13
Wet days vs. DJF ONI	-0.44**	-0.16

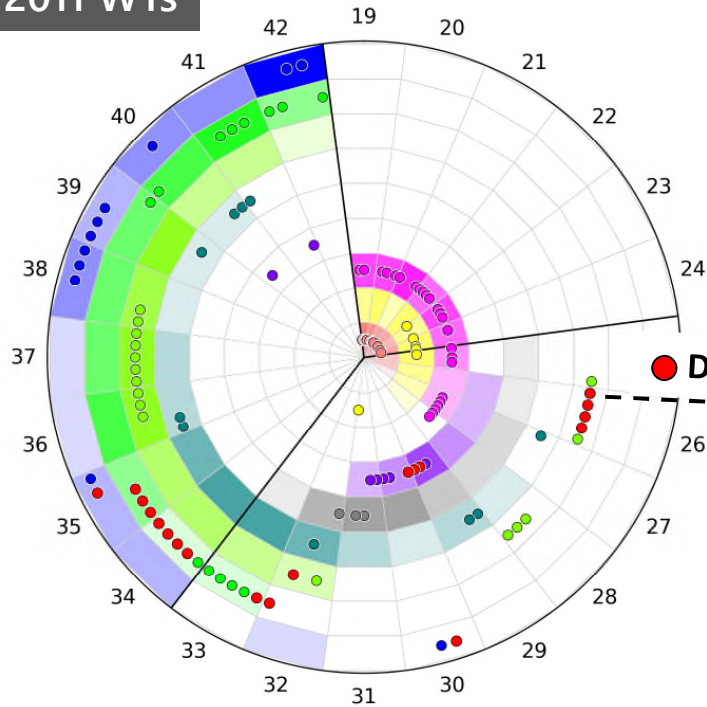
Wet Case – Philippines, 2011



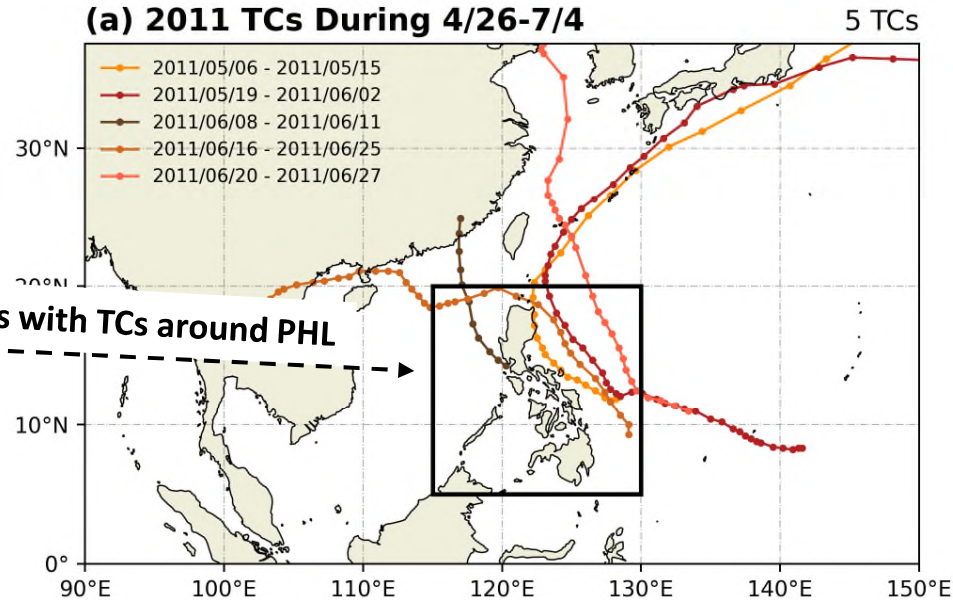
Dry Case – Taiwan, 2009



2011 WTs

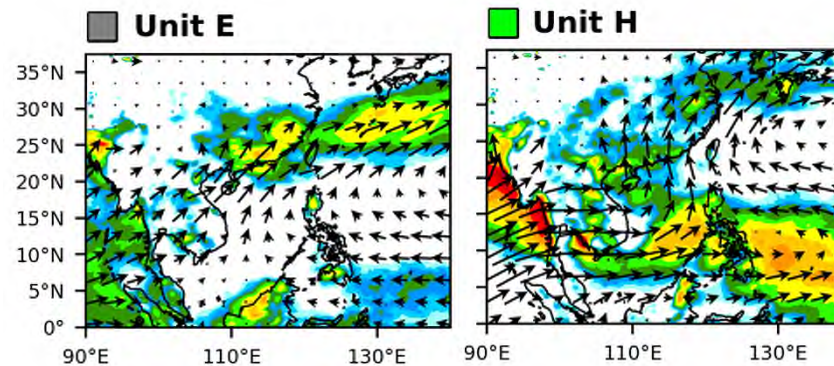
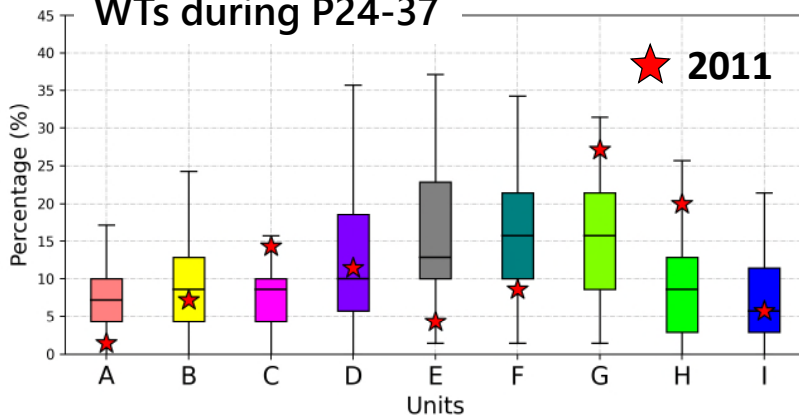


(a) 2011 TCs During 4/26-7/4



- Extreme wet event over the Philippines in 2011 can be reflected by active TCs around the Philippines, accompanied by less Unit E and more Unit H during 4/26-7/4.

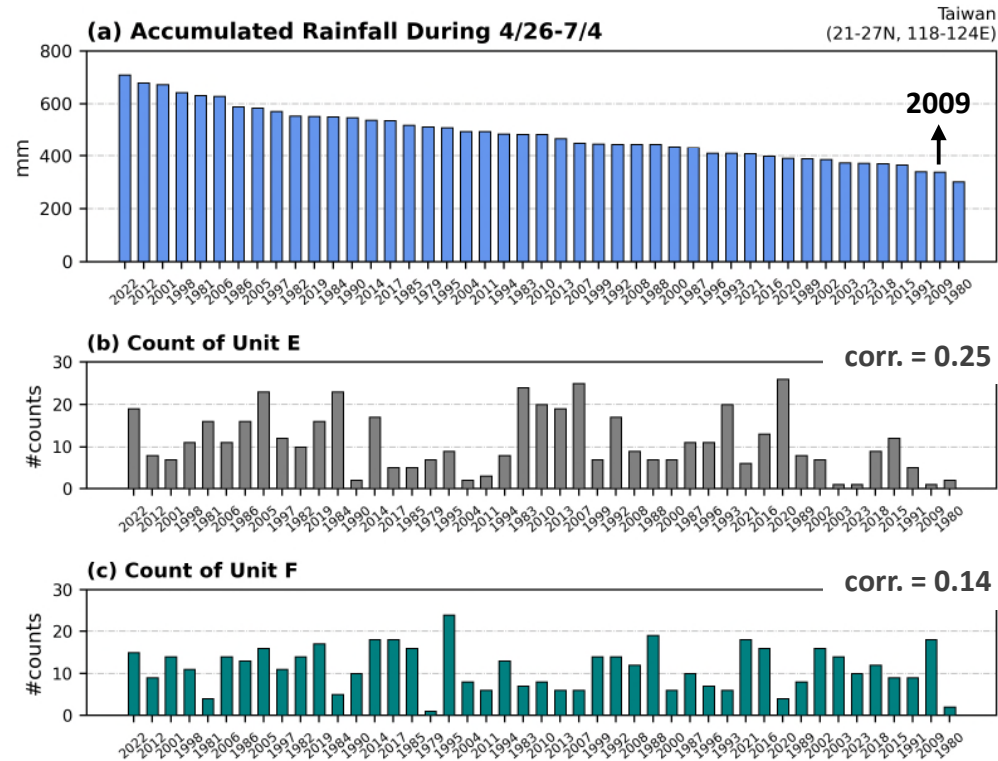
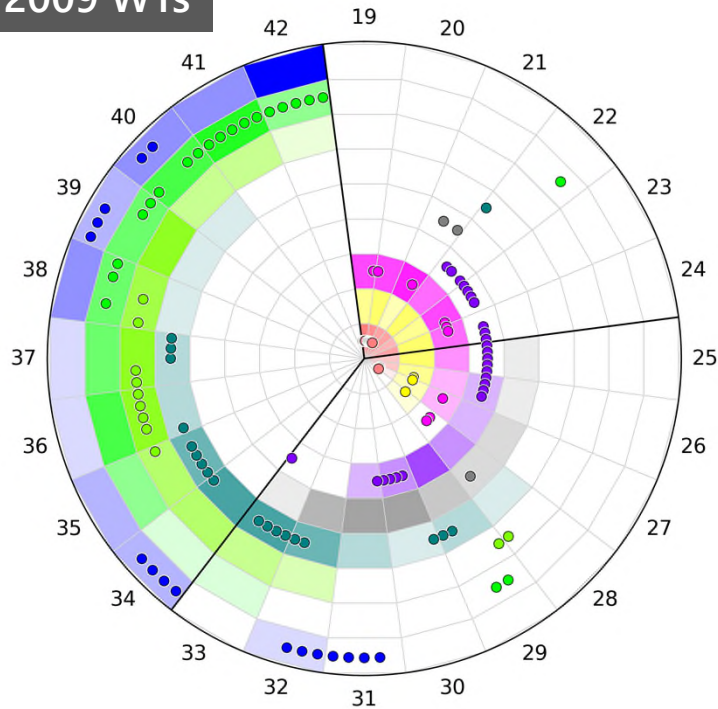
WTs during P24-37



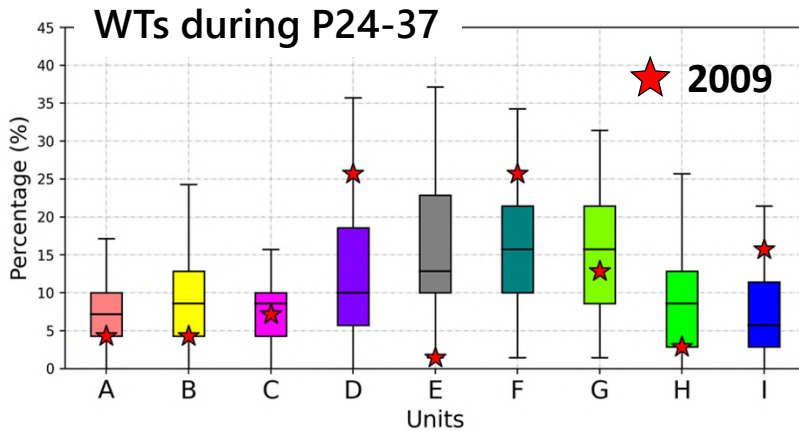
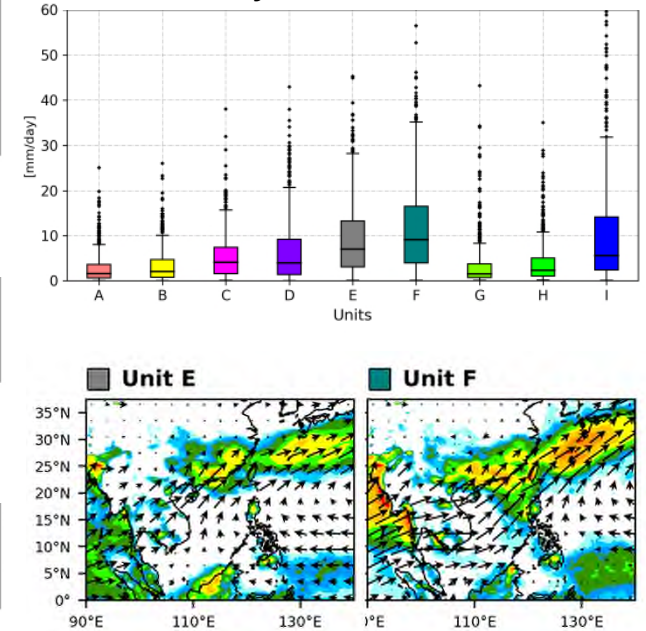
Corr. with accu. rainfall over PHL during 4/26-7/4

- Unit E = -0.46**
- Unit H = 0.4**

2009 WTs



ERA5 Daily Rainfall over Taiwan



- The dry case in 2009 may be related to the absence of Unit E.
- The occurrence of Units E and F cannot reflect the dry or wet condition over Taiwan during Mei-yu season in general.